

# POLITECNICO DI TORINO

MASTER's Degree in Automotive ENGINEERING



MASTER's Degree Thesis

Longitudinal and Vertical Dynamics Control in In-Wheel  
Motor Electric Vehicles

Supervisors

Prof. TONOLI ANDREA

Dr. SORRENTINO GENNARO

Dr. RAFFAELE MANCA

Candidate

MIAO YU

March 2025

## Abstract

With the increasing adoption of electric vehicles (EVs), in-wheel motor configurations have gained significant attention due to their potential for improved efficiency and controllability. This thesis focuses on the longitudinal dynamics of an in-wheel motor electric vehicle, where a comprehensive simulation model is developed to analyze vehicle behavior under different road conditions, such as bumps and slippery surfaces.

The developed model consists of a motor torque source, a road profile generator, and a quarter-car model that considers both longitudinal and vertical dynamics, through enveloping tire model. The system is first simulated without active control to establish baseline performance. A simple longitudinal controller is then introduced, employing a PID-based slip control mechanism that adjusts torque to regulate wheel slip. The impact of the controller on vehicle performance, including traction, stability, and ride comfort, is evaluated under different conditions. Key performance indicators such as road holding index, vertical acceleration, slip error integral, and maximum slip are analyzed to assess the effectiveness of the controller. The results demonstrate that the introduction of the traction control significantly enhances vehicle stability on slippery roads while having a minimal effect on ride comfort. The combined use of longitudinal and vertical controllers further improves comfort but introduces trade-offs in handling. These findings contribute to a better understanding of longitudinal control strategies for in-wheel motor electric vehicles and their real-world applicability.

## ACKNOWLEDGMENTS

I extend my highest respect to my parents for their unconditional support,  
to Italy for being the land that shaped me,  
to my tutors for their invaluable guidance,  
and to Charlotte for her presence in my journey.

# Table of Contents

<b>1</b>	<b>Introduction</b>	<b>1</b>
1.1	Background . . . . .	1
1.2	Research Objectives . . . . .	1
1.3	Structure of the Thesis . . . . .	1
<b>2</b>	<b>Literature Review</b>	<b>3</b>
2.1	Vehicle Dynamics in In-Wheel Motor EVs . . . . .	3
2.1.1	Impact of Increased Unsprung Mass on Ride Quality . . . . .	3
2.1.2	Importance of Longitudinal and Vertical Dynamics in Vehicle Performance . . . . .	5
2.1.3	Longitudinal Control Approaches . . . . .	10
2.2	Slip Control and PID Control . . . . .	10
2.2.1	Slip control . . . . .	10
2.2.2	PID control . . . . .	11
2.2.3	PID Relevance to Slip Control . . . . .	12
2.3	Vertical Control Strategies . . . . .	12
2.4	Introduction to Passive Dampers . . . . .	12
2.5	Skyhook Control Strategy . . . . .	13
<b>3</b>	<b>Methodology</b>	<b>15</b>
3.1	Overview . . . . .	15
3.2	Quarter-car Model . . . . .	15
3.2.1	Quarter-Car Model: Inputs and Outputs . . . . .	16
3.2.2	Applications . . . . .	18
3.3	Tire model . . . . .	20
3.3.1	Introduction to Pacejka 96 (Magic Formula) . . . . .	20
3.3.2	Pacejka 96 Equations (Magic Formula) . . . . .	20
3.3.3	Inputs and Outputs of the Pacejka 96 Model . . . . .	22
3.3.3.1	Inputs to the Pacejka 96 Model . . . . .	22
3.3.3.2	Outputs from the Pacejka 96 Model . . . . .	22
3.4	Controllers Design . . . . .	23
3.4.1	longitudinal controller . . . . .	23
3.4.2	Vertical controller . . . . .	25
3.5	Road Profiles and Simulation Scenarios . . . . .	26

3.5.1	ISO 8608 Class C road . . . . .	26
3.5.2	Three bumps . . . . .	26
3.5.3	Simulation Scenarios . . . . .	27
3.6	Road Profile Enveloping Model . . . . .	28
3.7	Key Performance Indicators (KPIs) . . . . .	29
3.7.1	Sprung-mass weighted vertical acceleration . . . . .	29
3.7.2	Road holding index . . . . .	29
3.7.3	Maximum slip . . . . .	29
3.7.4	Slip error integral . . . . .	30
<b>4</b>	<b>Results and Discussion</b>	<b>31</b>
4.1	KPI Analysis . . . . .	31
4.1.1	ISO class c road with constant friction coefficient ( testing influence of heavier unsprung mass ) . . . . .	31
4.1.1.1	Comfort Analysis . . . . .	33
4.1.1.2	Handling Performance . . . . .	33
4.1.1.3	Stability and Slip Control . . . . .	34
4.1.1.4	Necessity of Implications for TCS and Vertical Control Strategies . . . . .	34
4.1.2	ISO 8608 class c road with decreased friction coefficient ( $\mu$ ) . . . . .	34
4.1.2.1	Comfort Analysis . . . . .	35
4.1.2.2	Handling Performance . . . . .	35
4.1.2.3	Stability and Slip Control . . . . .	35
4.1.2.4	Conclusion . . . . .	35
4.1.3	Three bumps with decreased friction coefficient ( $\mu$ ) . . . . .	40
4.1.3.1	Comfort Analysis . . . . .	40
4.1.3.2	Handling Performance . . . . .	40
4.1.3.3	Stability and Slip Control . . . . .	41
4.1.3.4	Conclusions . . . . .	41
<b>5</b>	<b>Conclusion and future work</b>	<b>45</b>
5.1	Summary of Findings . . . . .	45
5.2	Future research directions . . . . .	45
5.2.1	Future Research Directions . . . . .	45
5.2.1.1	Development of More Complex and High-Fidelity Vehicle Models . . . . .	46
5.2.1.2	Advanced Control Strategies . . . . .	46
5.2.1.3	Integrated Longitudinal and Vertical Dynamics Control . . . . .	46
5.2.1.4	Experimental Validation and Real-Time Implementation . . . . .	47
5.2.1.5	Summary . . . . .	47
	<b>Bibliography</b>	<b>48</b>

# List of Figures

2.1	An In-wheel motor example [4]	7
2.2	(a) The body vertical vibration acceleration and (b) PSD curve when unsprung mass increases 20 kg [5]	8
2.3	(a) The body vertical vibration acceleration and (b) PSD curve when unsprung mass is initial value [5]	8
2.4	friction coefficient vs slip ratio [10]	10
3.1	model overview	15
3.2	Implemented model	16
3.3	quarter car model [6]	18
3.4	quarter model simulated in simulink	19
3.5	pachjka96 in simulink	21
3.6	Root Locus Plot of PID Controller	24
3.7	bode plot of the pid controller	24
3.8	Longitudinal controller	25
3.9	iso c class road profile	26
3.10	three bumps profile	27
3.11	zoomed in single bump	27
4.1	comparison of slip with and without IWM	32
4.2	comparison of sprung mass vertical acceleration with and without IWM	32
4.3	comparison of zu-w with and without IWM	33
4.4	slip of ISO C road with changing $\mu$	36
4.5	longitudinal speed of ISO class c road with changing $\mu$	37
4.6	longitudinal acceleration of slip of ISO C road with changing $\mu$	37
4.7	sprung mass vertical acceleration of ISO class c road with changing $\mu$	38
4.8	zu-w of ISO class c road with changing $\mu$	38
4.9	motor torque of ISO class c road with changing $\mu$	39
4.10	slip of three bumps with decreased friction coefficient	41
4.11	longitudinal speed of three bumps with decreased friction coefficient	42
4.12	longitudinal acceleration of three bumps with decreased friction coefficient	42
4.13	sprung mass vertical acceleration of three bumps with decreased friction coefficient	43

4.14	zu-w of three bumps with decreased friction coefficient . . . . .	43
4.15	motor torque of three bumps with decreased friction coefficient . . .	44

# List of Tables

3.1	Quarter-Car Model Inputs and Outputs . . . . .	18
3.2	Inputs to the Pacejka 96 Model . . . . .	22
3.3	Outputs from the Pacejka 96 Model . . . . .	22
4.1	Influence of performance of IWM . . . . .	31
4.2	Performance Comparison of Different Control Strategies . . . . .	35
4.3	Performance Comparison of Different Control Strategies on Road with Three Bumps and Variable Friction . . . . .	40

# Chapter 1

## Introduction

### 1.1 Background

In-wheel motors offer significant advantages for electric vehicles (EVs), including improved efficiency, space optimization, and enhanced control capabilities. However, their integration introduces challenges, particularly due to the increase in unsprung mass. This added mass affects ride comfort, handling, and stability, requiring counter strategies to reduce its negative impact.

### 1.2 Research Objectives

Because of the challenges posed by increased unsprung mass, this thesis focuses on developing and implementing a quarter-car model to analyze its effects. Specifically, the objectives include:

- Implementing a quarter-car model that considers in-wheel motors.
- Simulating the impact of unsprung mass on vehicle performance.
- Design and implement a simple anti-slip controller in combination with an active suspension (skyhook) to counteract its negative influence.

### 1.3 Structure of the Thesis

This thesis consists of five main chapters, each addressing a specific aspect of the research:

#### **Chapter 2: Literature Review**

This chapter reviews existing research and technical backgrounds on vehicle dynamics, and in-wheel motor electric vehicles. Focusing on their impact on vehicle dynamics. It also explores various control strategies for both longitudinal and vertical motion, providing a foundation for the proposed approach.

#### **Chapter 3: Methodology**

This chapter presents the development of the quarter-car model, detailing the mathematical formulations for vehicle dynamics. It also describes the tire model, the

design of a longitudinal controller, and the road profiles used in the simulations. Key performance indicators (KPIs) are introduced to evaluate the system's behavior.

**Chapter 4: Results and Discussion**

This chapter analyzes the simulation results, focusing on how different control methods influence vehicle performance. It evaluates the effectiveness of the control strategies in counter balancing the negative effects of increased unsprung mass. The impact of road conditions and other external influences is also discussed.

**Chapter 5: Conclusion and Future Work**

The final chapter summarizes the key findings of the research and discusses their implications. It also outlines potential areas for future work, including improvements in control strategies and extensions to more complex vehicle models.

# Chapter 2

## Literature Review

### 2.1 Vehicle Dynamics in In-Wheel Motor EVs

#### 2.1.1 Impact of Increased Unsprung Mass on Ride Quality

**Understanding Unsprung Mass:** In vehicle dynamics, unsprung mass refers to components not supported by the suspension, such as wheels, tires, brakes, and hubs (and in the case of in-wheel motors, the motor itself). By contrast, the sprung mass is the vehicle body and chassis, which are supported by springs and dampers. Lower unsprung mass has long been considered beneficial for ride and handling because the lighter the wheel assembly, the more easily the suspension can isolate the vehicle body from road bumps. When unsprung mass increases (for example, by adding heavy in-wheel motors), the wheel assemblies have greater inertia and are less able to follow road surface irregularities, which can transmit more shock and vibration to the cabin and compromise tire contact with the road.

**Effects on Ride Comfort:** Increased unsprung mass generally deteriorates ride comfort. A heavier wheel assembly tends to transmit more vertical acceleration to the sprung mass (vehicle body), making the ride feel harsher. Studies confirm that as unsprung weight grows, the vehicle's ride comfort (often measured by body acceleration) tends to decline[1]. This is because the suspension has a harder time isolating the cabin from road inputs. In a simple quarter-car model, the ratio of unsprung mass to sprung mass is a key factor influencing vibration transmissibility to the vehicle body. Essentially, a high unsprung/sprung mass ratio raises the acceleration response of the body over uneven roads. Experimental and simulation research backs this up: for instance, one study found that adding in-wheel motors (significantly increasing unsprung mass) led to higher root-mean-square (RMS) body acceleration, indicating a rougher ride[1]. Another detailed analysis showed that at higher speeds on a rough surface, doubling unsprung mass could raise peak body acceleration by over 10% Wu et al. (2024)[2], underscoring the impact on comfort.

**Effects on Handling and Roadholding:** Unsprung mass also strongly affects handling because it influences the tire's contact with the road. Automotive engineers have long warned that heavier unsprung components can degrade roadholding. When

a wheel encounters a bump, a lighter wheel can move up and down quickly, keeping the tire in contact with the road, whereas a heavier (high unsprung mass) wheel tends to lose contact or oscillate, reducing grip. This shows up in the metric of wheel dynamic load (the variation of tire force on the road). A higher unsprung mass causes larger fluctuations in tire forces, which can impair traction and stability. For example, researchers observed that increasing wheel mass significantly boosts the dynamic tire load; in one simulation, the peak tire force variation grew by up to 40% with heavier unsprung mass. (Shi et al., 2015)[1] Such an increase in tire load variation directly means worse road holding, especially in cornering or during quick transitions, as the tire may momentarily carry less load and thus less friction. Consequently, vehicles with heavy wheels (or in-wheel motors) can feel “bouncy” or less planted on uneven pavement, and may have longer stopping distances or reduced cornering grip on rough roads.

**In-Wheel Motors in EVs – Challenges and Findings:** In electric vehicles with in-wheel motors (IWMs), the motor adds a considerable amount of unsprung mass at each wheel. Early and foundational studies raised concerns that IWMs could hurt both ride comfort and handling. The primary concerns were that the added unsprung weight would degrade ride quality and road grip. Recent research has aimed to quantify and resolve these concerns with detailed models and real-world tests. For instance, Shi *et al.* (2015)[1] built a multi-body simulation of an EV with in-wheel motors and found a clear negative effect on ride comfort with increased unsprung mass. Their results showed higher body accelerations and suspension deflections when the motor mass was added, confirming the theoretical expectations. Similarly, Wu *et al.* (2024)[2] conducted a comprehensive evaluation using a full vehicle model and reported that, on random rough roads, adding unsprung mass (due to IWMs) enlarges wheel load fluctuations and suspension travel, thereby deteriorating both road-holding and ride performance. In that study, the heavier unsprung mass caused notably more oscillation in the tire forces and greater movement in the suspension, which translates to a less comfortable and less stable ride.

**Nuanced Effects and Mitigation:** Interestingly, recent findings also highlight that the impact of unsprung mass is not entirely one-dimensional. Wu *et al.* noted that the effect on vertical acceleration of the vehicle body can vary by location – for example, the front and rear of the vehicle experienced increased vibration with heavy unsprung wheels, but the center of the body showed a mix of increases and decreases at different speeds due to the “wheelbase filtering” effect (the spacing of front/rear wheels filtering out certain road wavelengths). They even found that a higher unsprung mass reduced body roll acceleration (body roll movement side-to-side) at all speeds, which could somewhat benefit handling in turns [2]. Moreover, on very bumpy roads, added unsprung mass had complex effects: it worsened all ride metrics at low vehicle speeds but improved some ride measures at high speeds on those same bumps[2]. These nuanced outcomes suggest that in certain conditions, a heavier wheel can damp out small high-frequency bumps (acting as a low-pass filter), albeit at the cost of worse performance in other regimes.

Crucially, modern engineering approaches can mitigate many of the downsides of increased unsprung mass. Suspension tuning and advanced dampers can be adjusted to compensate for heavier wheels. In fact, one wide-ranging study by Anderson and Harty[3] found that the ride and handling of a vehicle with in-wheel motors could be brought back near to normal by using the “modern development toolbox,” such as optimized suspension settings or even active control systems. Their tests, which included both subjective evaluations and objective measurements, showed that it’s possible to restore much of the lost dynamic performance with careful design adjustments. Researchers have proposed solutions like active and semi-active suspensions, or adding auxiliary mass dampers/inerters, specifically to counteract IWM-induced unsprung mass effects. These strategies aim to isolate the vehicle body from wheel disturbances or to better control wheel motions, thereby preserving ride quality and handling even with heavier in-wheel components.

In summary, increasing unsprung mass — such as by adding in-wheel motors in EVs — tends to negatively impact ride comfort and handling by transmitting more road shocks to the cabin and reducing tire contact consistency. Foundational vehicle dynamics theory and early studies warn of these effects, and recent research has quantified them (e.g., higher body accelerations and up to 40% greater tire force variation)[2] . However, contemporary engineering research also shows that with innovative suspension design and control, the adverse impacts can be minimized or managed. Automotive engineers must account for the trade-off: while in-wheel motors offer advantages (like more space and direct wheel control), their added unsprung weight requires careful suspension optimization to maintain a comfortable ride and safe, predictable handling. (Shi et al., 2015; Wu et al., 2024; Anderson & Harty, 2010)[2][1][3]

### **2.1.2 Importance of Longitudinal and Vertical Dynamics in Vehicle Performance**

Vehicle performance is highly influenced by longitudinal dynamics and vertical dynamics, which are especially critical for electric vehicles (EVs) with in-wheel motors. Longitudinal dynamics refers to acceleration and braking along the direction of travel, directly affecting traction, acceleration times, and braking distances. Vertical dynamics describes the up-and-down motion of the vehicle’s sprung and unsprung masses (the suspension movement) as it responds to road irregularities, influencing ride comfort and tire contact with the road. Both aspects are fundamental to overall vehicle behavior and safety, and they often interact. For instance, road bumps induce vertical oscillations that can lead to fluctuations in wheel loads and longitudinal acceleration, impacting ride comfort and stability . Understanding and optimizing these dynamics is crucial for any vehicle, and new EV technologies bring both challenges and opportunities in this area.

#### **Longitudinal Dynamics and Vehicle Performance**

Effective longitudinal dynamics ensure that a vehicle can accelerate and decelerate

predictably while maintaining traction. This involves managing weight transfer and tire slip during acceleration or braking. Good longitudinal performance means the car can put power to the ground without excessive wheel spin and can brake without wheel lock-up, maintaining stability. In EVs, the instant torque from electric motors can improve longitudinal response, but it also demands sophisticated control to prevent tire slip. Particularly in vehicles with in-wheel motors (where each wheel has its own motor), independent torque control at each wheel can be used to enhance traction and stability. Because each in-wheel motor can be controlled separately, advanced algorithms (like torque vectoring or individual wheel slip control) can optimize longitudinal force distribution for acceleration and braking on the fly . This capability gives EVs with in-wheel drives unprecedented flexibility to achieve optimal longitudinal performance. However, maximizing the benefit requires careful coordination with the vehicle’s vertical dynamics, as wheel load variations from bumps or body pitch will affect how much longitudinal force each tire can generate.

### **Vertical Dynamics and Vehicle Performance**

Vertical dynamics primarily affect ride comfort and the consistency of tire forces on the road. A car’s suspension is designed to absorb road unevenness (improving *ride* comfort) while maintaining tire contact for *handling* and traction. It is well established that unsprung mass – the mass of components like wheels, tires, and in-wheel motors that is not supported by the suspension – is a key factor in vertical dynamic behavior . Higher unsprung mass generally leads to poorer ride quality and can reduce the tire’s ability to follow road contours, which in turn can degrade handling. In fact, increasing unsprung mass tends to worsen vehicle dynamics if not compensated . For example, a heavier wheel assembly will transmit more bump energy to the chassis, causing discomfort and possibly momentary loss of tire grip. Therefore, keeping unsprung mass low is traditionally a goal to enhance both comfort and road holding.

At the same time, modern suspension design and control systems can mitigate many negative effects. Anderson and Harty (2010)[3] observed that with today’s “development toolbox” (such as adaptive dampers and careful tuning), it is possible to restore dynamic performance even when unsprung mass is increased . In their study, a test vehicle with significantly added wheel mass still achieved comparable ride and handling to a standard setup after re-tuning the suspension, highlighting that engineering measures can compensate for higher unsprung weight. In essence, vertical dynamics must be finely managed to ensure the vehicle remains comfortable and the tires maintain consistent contact with the road, which also supports strong longitudinal performance (since a tire can only provide traction when it is firmly in contact with the road surface).

### **Implications for EVs with In-Wheel Motors**

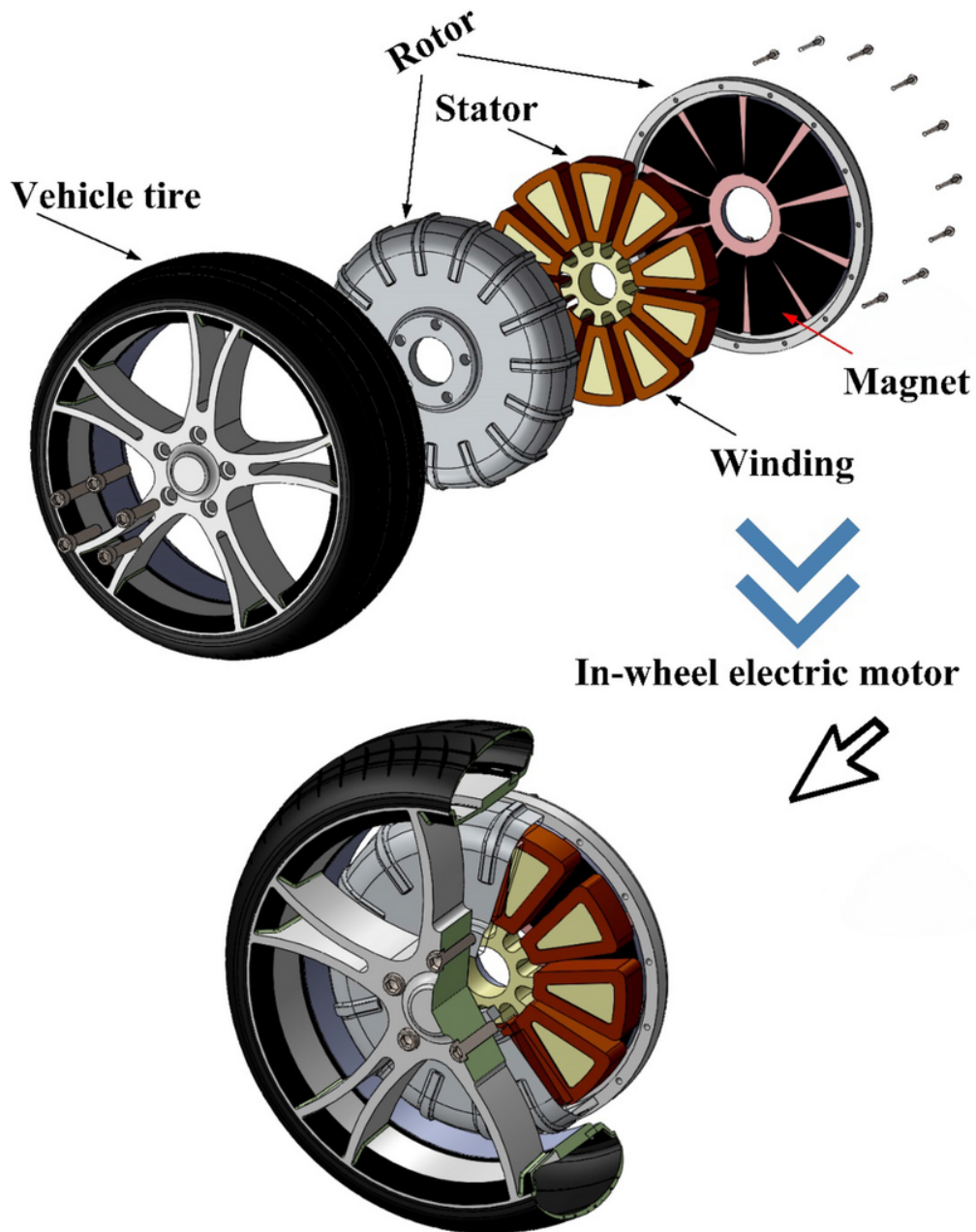


**Figure 2.1:** An In-wheel motor example [4]

In EVs featuring in-wheel motors, longitudinal and vertical dynamics become even more intertwined. In-wheel motors add to the unsprung mass, since the motor's weight is located in the wheel itself. This inherently poses a challenge: the added unsprung mass can degrade ride comfort and road holding if left unaddressed. Studies have identified unsprung mass as one of the most critical drawbacks of in-wheel drive designs. For instance, Jin et al. (2016) [5] demonstrated that the ratio of unsprung to sprung mass has a significant impact on ride comfort in vehicles driven by in-wheel motors. A higher ratio (meaning relatively heavier wheels) tends to increase vibration levels felt in the cabin, confirming the importance of minimizing unsprung weight or counteracting its effects. Furthermore, vertical vibrations due to road irregularities can cause fluctuations in wheel speed and traction in an in-wheel

motor system. Without intervention, a bump in the road might induce a momentary longitudinal acceleration oscillation as the wheel hops and regains grip .

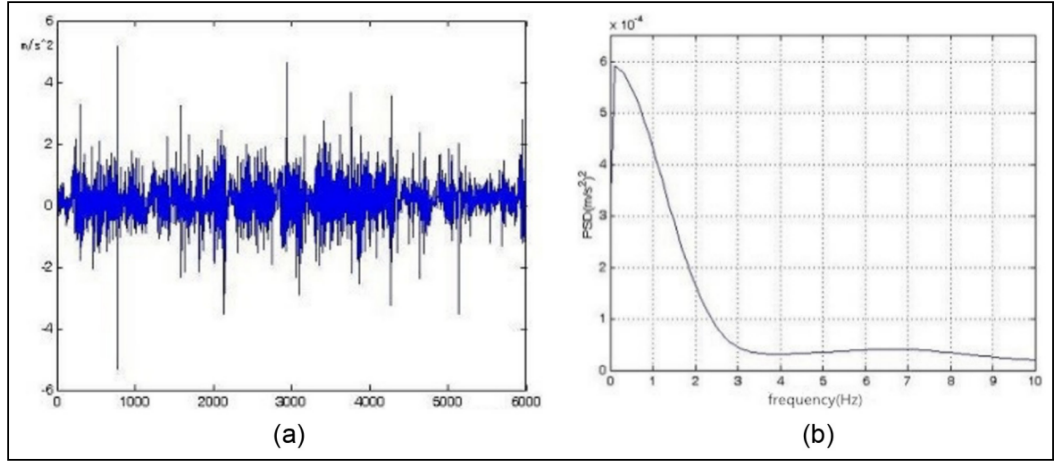


**Figure 2.2:** (a) The body vertical vibration acceleration and (b) PSD curve when unsprung mass increases 20 kg [5]

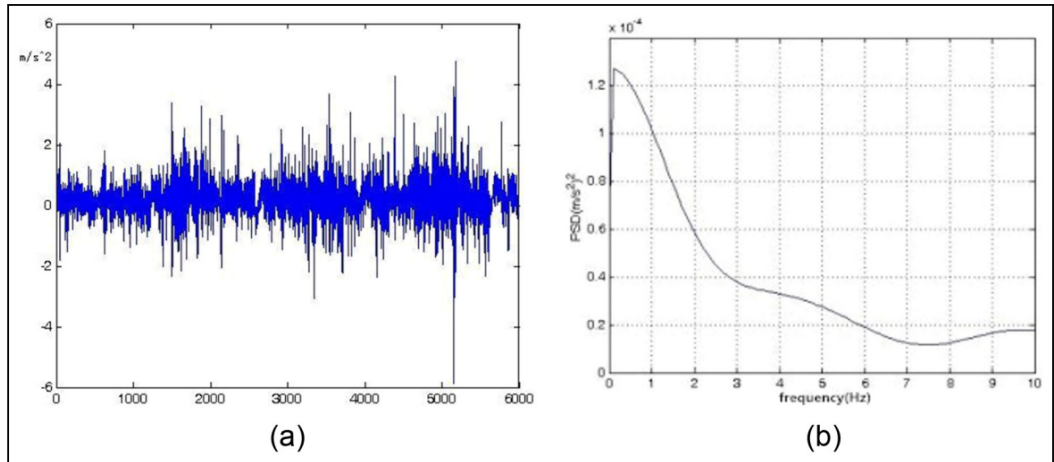


**Figure 2.3:** (a) The body vertical vibration acceleration and (b) PSD curve when unsprung mass is initial value [5]

Despite these challenges, in-wheel motor EVs also offer unique opportunities to enhance performance through integrated control of longitudinal and vertical dynamics. The independent motors at each wheel can react rapidly to changing conditions. Researchers have proposed strategies to exploit this, such as using the motors for *active vibration control*. For example, a coupled longitudinal-vertical dynamic model was used to design a dynamic vibration absorption approach in an EV, which effectively reduced vibrations by using the in-wheel motor system itself as part of the damping mechanism . Similarly, Vidal *et al.* (2022)[6] introduced a pre-emptive control scheme where each in-wheel motor adjusts its torque based on upcoming road profile information, aiming to reduce the oscillations in longitudinal acceleration caused by road bumps . This kind of predictive *road-adaptive traction control* can improve ride comfort and stability by momentarily limiting or modulating

torque when a wheel is about to hit a bump, then reapplying power when contact is re-stabilized. Such advanced control approaches highlight how tightly coupled the longitudinal and vertical dynamics are in these vehicles and how one can compensate for the other.

In addition to electronic control solutions, mechanical improvements can help as well. Specialized suspension designs for in-wheel motor setups have been shown to regain much of the lost ride quality. For instance, adding a lightweight suspension module for the in-wheel motor (essentially isolating the motor's mass from the main suspension) was found to improve ride comfort by around 8–9% in terms of vibration metrics . Also, new suspension control strategies have been tested: one study combined an active suspension with a tuned mass damper attached to the wheel assembly, and reported notable reductions in vibration and improved comfort in an in-wheel motor EV . These findings suggest that while in-wheel motors introduce vertical dynamic challenges, engineering solutions (both mechanical and electronic) can address them effectively.

Overall, the importance of longitudinal and vertical dynamics in vehicle performance is undeniable, and it is amplified in EVs with in-wheel motors. Longitudinal dynamics ensure the EV can accelerate and brake efficiently, but without good vertical dynamics, the tires may not stay planted to use that power or braking force. Conversely, poor longitudinal control (like excessive wheel slip) can exacerbate vertical bouncing by generating uneven tire forces. Thus, designers of modern electric vehicles, especially those with in-wheel propulsion, must consider longitudinal and vertical dynamics in tandem. By leveraging the precise motor control and developing suspensions that cope with higher unsprung mass, automakers and researchers aim to achieve a balance where the vehicle can deliver strong acceleration and braking while maintaining a smooth, stable ride. This balance leads to better overall performance, safety, and comfort, fulfilling the promise of in-wheel motor technology without sacrificing traditional dynamic qualities . (Anderson & Harty, 2010; Jin et al., 2016; Qin et al., 2018; Quynh et al., 2019; Vidal et al., 2022; Deepak et al., 2023)[3][5][7][8] [6][9]

### 2.1.3 Longitudinal Control Approaches

## 2.2 Slip Control and PID Control

### 2.2.1 Slip control

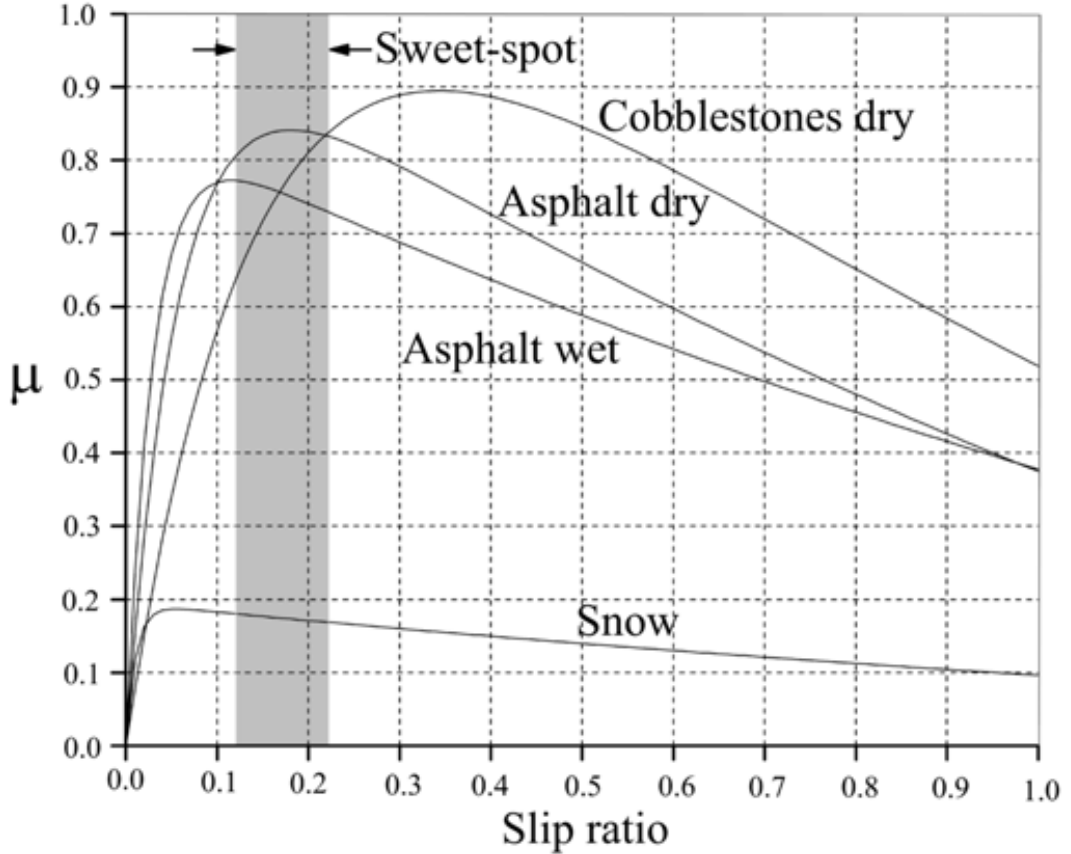


**Figure 2.4:** friction coefficient vs slip ratio [10]

Controlling wheel slip is crucial for maximizing tire-road friction and maintaining stability during braking or acceleration. The friction coefficient between tire and road typically peaks at a moderate slip ratio (often around 10–30%, depending on surface) [11]. In practice, many anti-lock braking and traction control systems aim to maintain slip around 0.2 (20%) where friction is near its maximum, ensuring shorter stopping distances and good vehicle control [11].

Various control methodologies have been developed to regulate wheel slip at or near this optimal value, even as road conditions change:

- **Threshold/Bang-Bang Control:** Early ABS systems used on-off modulation of brake pressure. They release the brake when wheel deceleration or slip exceeds a threshold, then reapply when the wheel regains traction.
- **PID/PI Slip Controllers:** A classical approach is to use a feedback controller (e.g., Proportional–Integral or PI) to track a desired slip ratio. The controller continuously adjusts brake torque or engine torque based on slip error.

- **Robust Nonlinear Control:** Modern strategies use nonlinear and robust control techniques (sliding mode, optimal control, etc.) to handle the highly nonlinear tire dynamics [12].
- **Adaptive Slip Control (Friction Estimation):** In adaptive schemes, the controller actively estimates the current friction coefficient ( $\mu$ ) and adjusts the target slip or control policy accordingly [13].

### 2.2.2 PID control

PID control stands for Proportional–Integral–Derivative control, a widely used feedback control strategy in engineering. A PID controller continuously calculates an error (the difference between a desired setpoint and the measured process variable) and adjusts the control input to minimize this error. It consists of three terms:

Proportional (P)

$$u_P = K_P \cdot e(t) \quad (2.1)$$

The P-action provides an immediate corrective effort – for slip control, if wheel slip error is positive (slip too high), the P-term might reduce drive torque or increase brake pressure proportionally to counteract the slip deviation. Higher  $K_P$  means a stronger reaction to errors, but too high can cause oscillations.

Integral (I)

$$u_I = K_I \int_0^t e(\tau) d\tau \quad (2.2)$$

The integral term responds to the accumulation of past error. It addresses systematic bias or steady-state errors. In a slip control context, even if a small slip error persists (perhaps due to a slight mismatch in friction), the I-term will gradually build up to eliminate that error, ensuring the long-term average slip reaches the target. However, excessive integral action can lead to overshoot or a sluggish response if not tuned well.

Derivative (D)

$$u_D = K_D \frac{d}{dt} e(t) \quad (2.3)$$

This anticipates where the error is heading by damping the controller output in response to rapid changes. In vehicle slip control, the D-term can help prevent the slip ratio from changing too quickly (e.g., wheel slip spiking when hitting an icy patch) by tempering the control input. Essentially, it adds stability and reduces overshoot by reacting to the slope of the error curve.

Total PID Output

$$u(t) = u_P + u_I + u_D = K_P e(t) + K_I \int_0^t e(\tau) d\tau + K_D \frac{d}{dt} e(t) \quad (2.4)$$

Tuning the gains ( $K_P, K_I, K_D$ ) is critical: for slip control, a well-tuned PID can smoothly maintain the desired slip ratio. If tuned poorly, it could either respond too slowly (allowing excessive slip) or too aggressively (causing oscillation between

slipping and gripping).

### 2.2.3 PID Relevance to Slip Control

PID controllers are popular in vehicle control systems due to their simplicity and effectiveness. For wheel slip control, a PID (or often PI) controller can be used to track the slip ratio setpoint (which might be fixed or provided by an adaptive scheme). For example, given a desired slip of 15%, a PID controller would adjust the brake or engine torque based on the slip error. The proportional part provides immediate correction if slip deviates, the integral part ensures zero steady-state error (so the slip stays exactly at 15% in the long run), and the derivative part helps prevent oscillatory behavior like wheel hop or repeated excessive slipping.

One practical consideration is that the optimal slip target can change with road conditions, as discussed above. A pure PID doesn't account for changing friction on its own – it will try to drive the slip to whatever setpoint it's given. That's why PID is often combined with the adaptive strategies: for instance, the system may use friction estimation to update the slip setpoint, and then a PID loop executes that setpoint. In some designs, gain scheduling is applied to the PID itself: the PID gains might be tuned differently for dry vs. slippery roads to account for differences in dynamics. Despite the rise of advanced control methods, PID (and PI) controllers remain a relevant baseline and are even used in production traction control systems due to their robustness, ease of implementation, and the intuitive understanding they provide in managing slip.

In summary, PID control provides a straightforward way to regulate wheel slip by continuously correcting the error between desired and actual slip. When incorporated into a larger slip control scheme (potentially with adaptive slip targets), a PID-controlled system can effectively keep the tire at its friction sweet spot, thereby enhancing vehicle safety and performance in varying driving conditions.

## 2.3 Vertical Control Strategies

### 2.4 Introduction to Passive Dampers

Passive dampers are suspension components that dissipate vibrational energy as heat, typically using viscous fluid friction. They provide a resistive force proportional to the relative velocity across the damper:

$$F_d = c \Delta \dot{x}, \quad (2.5)$$

where  $c$  is the damping coefficient and  $\Delta \dot{x}$  is the relative velocity [14].

In a simple mass-spring-damper system, the equation of motion is

$$m\ddot{x} + c\dot{x} + kx = 0, \quad (2.6)$$

where  $m$  is the mass,  $k$  the spring stiffness, and  $c$  the damping coefficient. The damping ratio  $\zeta = \frac{c}{2\sqrt{mk}}$  characterizes the damping level [14]. When  $c$  equals the critical damping value  $c_{\text{crit}} = 2\sqrt{mk}$  (i.e.  $\zeta = 1$ ), the system is *critically damped* and returns to equilibrium without oscillation. If  $c$  is lower ( $\zeta < 1$ , underdamped), the system exhibits oscillatory decay; if  $c$  is higher ( $\zeta > 1$ , overdamped), the return to equilibrium is slower.

In vehicle suspension design, passive dampers must be tuned as a compromise between ride comfort and road holding. A higher damping coefficient yields quick dissipation of oscillations (improving stability), but transmits more shock to the vehicle body. Conversely, lower damping improves vibration isolation (comfort) but allows larger oscillations and body motion [15]. This inherent compromise means a fixed-coefficient passive damper cannot optimally adapt to all road and load conditions.

## 2.5 Skyhook Control Strategy

The *skyhook* control strategy is a classic semi-active damping approach introduced by Karnopp *et al.* in the 1970s [16]. The concept is to emulate an ideal damper connecting the sprung mass (vehicle body) to an immobile reference point (the “sky”). An ideal skyhook damper would exert a force

$$F_{\text{sky}} = -C_s \dot{z}_s, \quad (2.7)$$

on the vehicle body, proportional to its velocity  $\dot{z}_s$  relative to an inertial reference (the sky) [16]. This hypothetical damper directly dissipates the body’s motion without affecting wheel movement.

Since a physical damper cannot be attached to a fixed point in space, skyhook control is implemented by modulating a real damper between the vehicle’s sprung and unsprung masses. The damper’s effective coefficient is varied in real time to approximate the skyhook effect [16]. Karnopp’s original formulation uses a simple on-off control law. Specifically, when the sprung mass and the suspension (sprung–unsprung) are moving in the same direction (i.e.  $\dot{z}_s(\dot{z}_s - \dot{z}_u) > 0$ ), a high damping  $C_{\text{max}}$  is applied. When they move in opposite directions ( $\dot{z}_s(\dot{z}_s - \dot{z}_u) < 0$ ), a low damping  $C_{\text{min}}$  is used. This rule ensures the damper produces force to oppose the sprung mass velocity only when it would dissipate energy from the body, thus mimicking the skyhook damper [16].

The skyhook strategy significantly improves ride comfort and vehicle stability compared to a purely passive damper. By effectively damping the sprung mass relative to an inertial frame, it reduces the body acceleration and resonance, leading to a smoother ride. At the same time, it avoids unnecessary high damping on the wheel, thus maintaining better tire contact with the road over bumps [15]. Classic studies have shown that a semi-active skyhook suspension can achieve much of the vibration reduction benefit of a fully active suspension, while using only modulated

passive elements and requiring no substantial external power input [16, 15].

# Chapter 3

## Methodology

### 3.1 Overview

In this thesis, a Simulink model is implemented to simulate the effect of the unsprung mass and evaluate the effectiveness of the developed controllers, and it consists of a motor torque source (a step input), road profile generator, a quarter car model (including tire model), the detailed explanation is illustrated in the sections after.

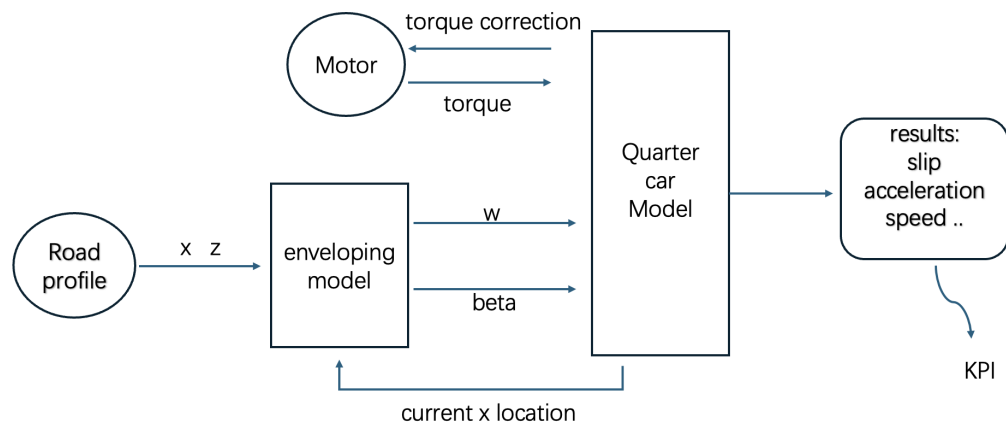


Figure 3.1: model overview

### 3.2 Quarter-car Model

The Quarter-Car Model is a simplified representation of a vehicle's suspension system, focusing on a single wheel and its interaction with the vehicle body and road surface. It is widely used in ride comfort, handling, and tire-road interaction analysis. The model is made of a sprung mass (vehicle body) and an unsprung mass (wheel assembly), connected by a suspension system with springs and dampers. The unsprung mass also connected longitudinally to the Mapp. External forces such as road irregularities, rolling resistance, and aerodynamic drag influence the system's behavior. In this thesis at later stage anactive force is implemented between  $M_u$  and  $M_b$ . In the quarter model  $F_x$  is coming from pachjka96 model.

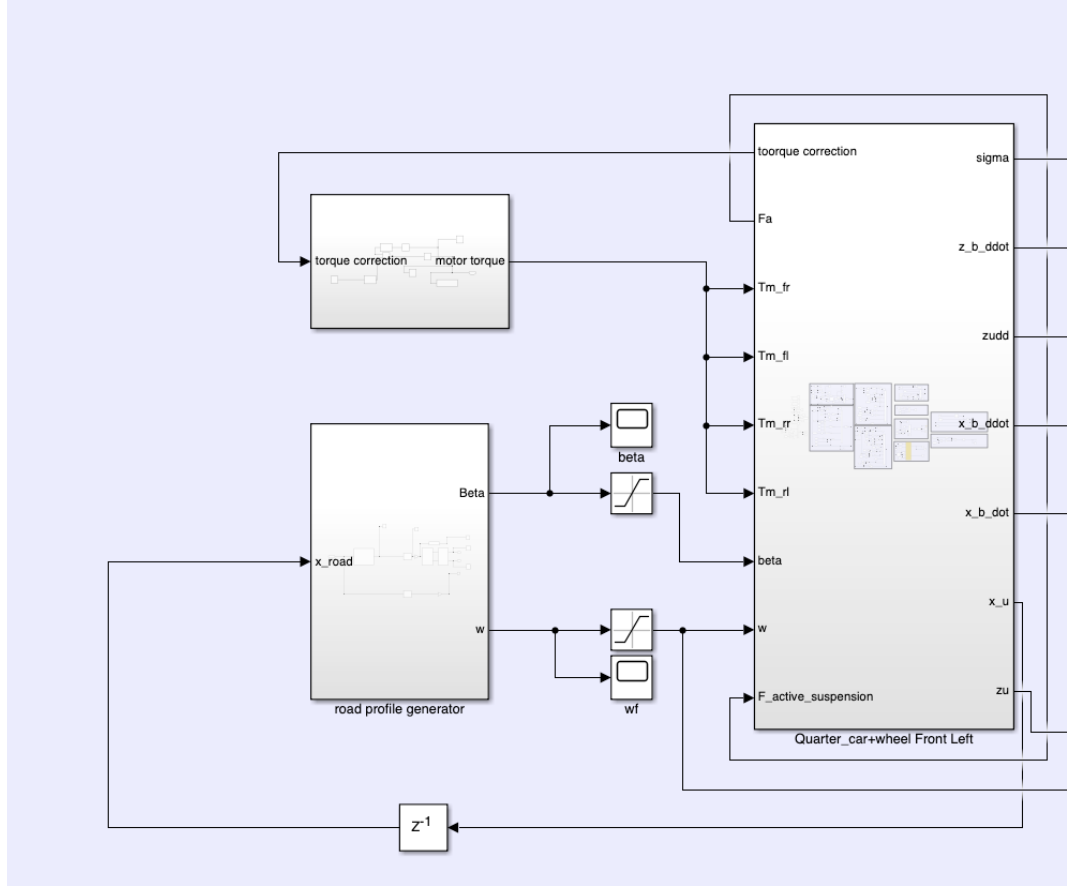


Figure 3.2: Implemented model

### 3.2.1 Quarter-Car Model: Inputs and Outputs

#### Inputs of the Quarter-Car Model

The model takes various external forces and parameters as inputs:

##### (a) Road Profile Input

- $W_r$  : Road surface height variations (bumps, potholes).
- $\beta$  : Inclination angle of the road, affecting both longitudinal and vertical forces.

##### (b) Longitudinal and Vertical Forces

- $F_x$  : Longitudinal tire force (traction/braking).
- $F_z$  : Vertical tire force.
- $F_k$  : Suspension spring force.
- $F_c$  : Suspension damping force.

**(c) In-Wheel Motor Torque**

- $T_m$  : Torque applied by the in-wheel motor, influencing acceleration and slip ratio.

**(d) Vehicle and Suspension Parameters**

- $m_s, m_u$  : Sprung and unsprung mass.
- $k_s, c_s$  : Suspension stiffness and damping.
- $k_r, c_r$  : Tire stiffness and damping.
- $F_{\text{drag}}$  : Aerodynamic drag force.
- $F_{\text{roll}}$  : Rolling resistance force.

**Outputs of the Quarter-Car Model**

The model provides various outputs describing vehicle and tire dynamics:

**(a) Sprung Mass Responses**

- $z_b$  : Vertical displacement of the vehicle body.
- $\dot{z}_b$  : Vertical velocity of the sprung mass.
- $\ddot{z}_b$  : Vertical acceleration, affecting ride comfort.

**(b) Unsprung Mass Responses**

- $z_u$  : Vertical displacement of the wheel assembly.
- $\dot{z}_u$  : Vertical velocity, used to evaluate tire-road contact stability.

**(c) Longitudinal Dynamics**

- $x_b$  : Longitudinal displacement of the vehicle.
- $\dot{x}_b$  : Vehicle velocity.
- $\ddot{x}_b$  : Longitudinal acceleration, influencing traction and braking.

**(d) Tire Slip and Contact Forces**

- $\kappa$  : Slip ratio, determining traction and grip.
- $F_x, F_z$  : Tire-road interaction forces.
- $\omega$  : Wheel angular velocity.

Inputs	Outputs
$W_r, \beta$	$z_b, \dot{z}_b, \ddot{z}_b$
$F_k, F_c$	$z_u, \dot{z}_u$
$F_x, F_z$	$x_b, \dot{x}_b, \ddot{x}_b$
$T_m$	$\kappa, \omega$
$F_{\text{drag}}, F_{\text{roll}}$	Tire-road contact forces

Table 3.1: Quarter-Car Model Inputs and Outputs

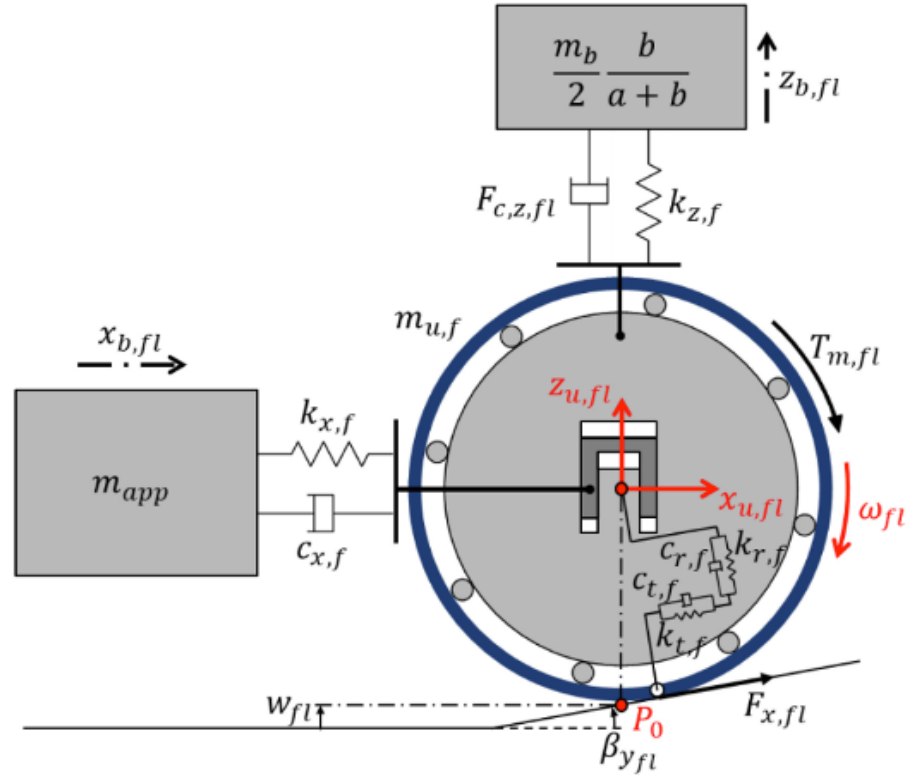
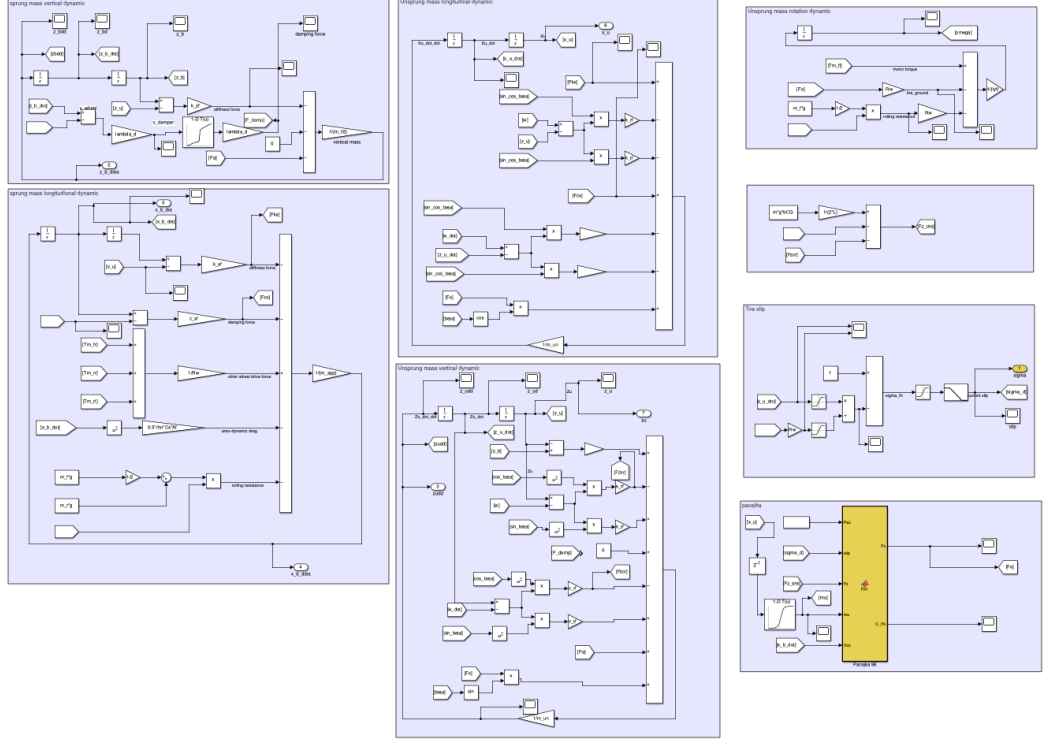


Figure 3.3: quarter car model [6]

### 3.2.2 Applications

- **Ride Comfort Analysis:** Evaluates vertical acceleration of the sprung mass. Kpis: sprungmass vertical acceleration.
- **Vehicle Handling Study:** Examines how forces affect tire-road grip and slip ratio. RHI( road hodling index)

Quarter-Car Model Equations



**Figure 3.4:** quarter model simulated in simulink

Sprung Mass Vertical Motion

$$\dot{Z}_b = \frac{1}{m_s} (-F_{kz} - F_{cz}) \quad (3.1)$$

$$F_{kz} = k_{zf}(z_b - z_u) \quad (3.2)$$

$$F_{cz} = c_{zf}(\dot{Z}_b - \dot{Z}_u) \quad (3.3)$$

Sprung Mass Longitudinal Motion

$$\dot{X}_b = \frac{1}{m_{app}} \left[ -F_{kx} - F_{cx} + \frac{T_{m,frl}}{R} + \frac{T_{m,rrl}}{R} - F_{drag} - F_{roll} \right] \quad (3.4)$$

$$F_{kx} = k_{xf}(X_b - X_u) \quad (3.5)$$

$$F_{cx} = c_{xf}(\dot{X}_b - \dot{X}_u) \quad (3.6)$$

$$F_{drag} = \frac{1}{2} \rho C_d A_f \dot{X}_b^2 \quad (3.7)$$

$$F_{roll} = \left( \frac{m_r g}{2} + m_{rear g} \right) f_{roll} \quad (3.8)$$

Unsprung Mass Vertical Motion

$$\ddot{Z}_u = \frac{1}{m_u} \left[ F_{kz} - k_{r,f}(Z_u - W_f) \cos^2(\beta) + k_{t,f}(Z_u - W_f) \sin^2(\beta) - c_{r,f}(\dot{Z}_u - \dot{W}_f) \cos^2(\beta) + c_{t,f}(\dot{Z}_u - \dot{W}_f) \sin^2(\beta) + F_{cz} + F_x \sin(\beta) \right] \quad (3.9)$$

Unsprung Mass Longitudinal Motion

$$\ddot{X}_u = \frac{1}{m_u} \left[ F_{kx} + F_{cx} + k_{r,f}(Z_u - W_f) \sin(\beta) \cos(\beta) + k_{t,f}(Z_u - W_r) \sin(\beta) \cos(\beta) + c_{r,f}(\dot{Z}_u - \dot{W}_f) \sin(\beta) \cos(\beta) + c_{t,f}(\dot{Z}_u - \dot{W}_f) \sin(\beta) \cos(\beta) + F_x \cos(\beta) \right] \quad (3.10)$$

Wheel Rotation Equation

$$\dot{\omega} = \frac{1}{I_y} \left[ T_{fl} - F_x R - \left( \frac{mg}{2} f_{\text{roll}} R \right) \right] \quad (3.11)$$

### 3.3 Tire model

#### 3.3.1 Introduction to Pacejka 96 (Magic Formula)

The Pacejka 96 tire model, also called the Magic Formula, is a semi-empirical model. It describes tire forces under different slip conditions. Hans B. Pacejka developed it. This model gives a mathematical way to show longitudinal force, lateral force, and aligning moment based on tire data.

Unlike models based only on physics, the Magic Formula is made to match non-linear tire behavior using adjustable coefficients. These coefficients are set to fit real tire data. This makes the model very accurate for vehicle dynamics simulations.

Key Features of Pacejka 96 are shown in the following

Nonlinear behavior: Shows how tire forces change with slip. Works for many cases: Used for braking, acceleration, cornering, and aligning moment. Adjustable parameters: Coefficients can change for different tires, road conditions, and uses. Common in simulations: Used in motorsports, car development, and driving simulators. Applications of the Pacejka 96 Model: Vehicle dynamics study: Helps understand how tires affect stability and handling. Traction control and ABS: Used in car safety systems. Suspension and chassis tuning: Helps improve ride and handling. Motorsport and racing: Used to improve tire performance for racing.

Limitations: Needs test data: Requires experiments to set parameters. Not fully physics-based: Does not directly explain tire mechanics. Less accurate in extreme cases: May not work well for very high slip angles (like drifting) or off-road driving.

#### 3.3.2 Pacejka 96 Equations (Magic Formula)

General Magic Formula

$$Y = D \sin \left( C \tan^{-1} \left( BX - E(BX - \tan^{-1}(BX)) \right) \right) \quad (3.12)$$

Longitudinal Force Equation (Braking & Acceleration)

$$F_x = D_x \sin \left( C_x \tan^{-1} \left( B_x \kappa - E_x(B_x \kappa - \tan^{-1}(B_x \kappa)) \right) \right) \quad (3.13)$$

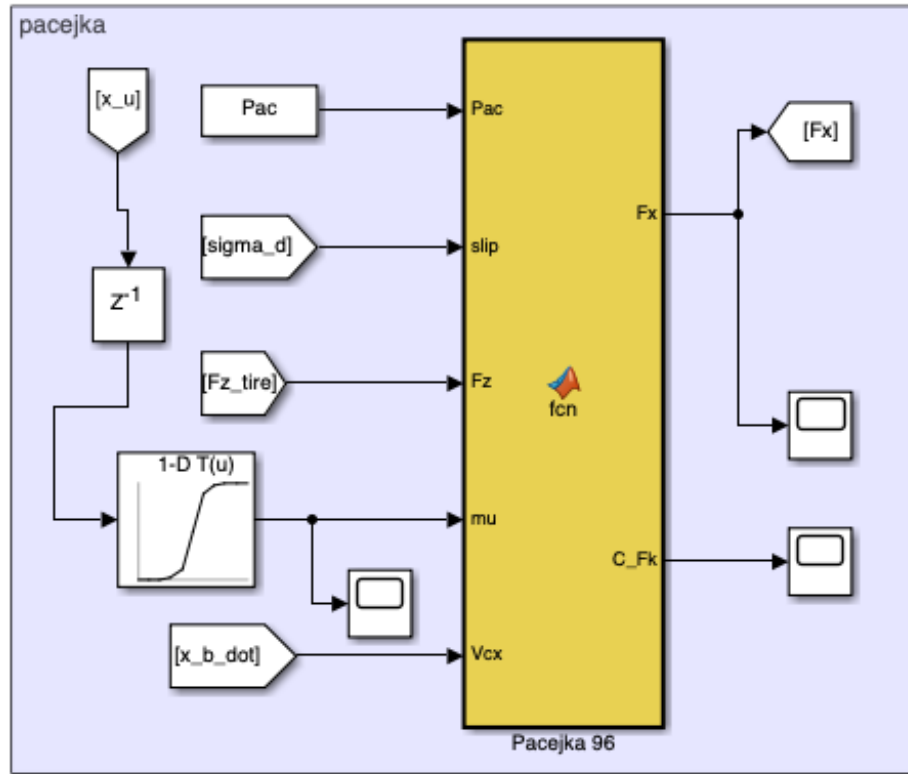


Figure 3.5: pachjka96 in simulink

Lateral Force Equation (Cornering Behavior)

$$F_y = D_y \sin \left( C_y \tan^{-1} \left( B_y \alpha - E_y (B_y \alpha - \tan^{-1}(B_y \alpha)) \right) \right) \quad (3.14)$$

Aligning Moment Equation (Self-Aligning Torque)

$$M_z = D_z \sin \left( C_z \tan^{-1} \left( B_z \alpha - E_z (B_z \alpha - \tan^{-1}(B_z \alpha)) \right) \right) \quad (3.15)$$

#### Explanation of Variables

- Y = General output (tire force or moment)
- X = Input variable (slip ratio  $\kappa$  or slip angle  $\alpha$ )
- B = Stiffness factor
- C = Shape factor
- D = Peak factor
- E = Curvature factor

In this thesis only the first two equations are used. Cause in the simulation only longitudinal behavior is considered.

### 3.3.3 Inputs and Outputs of the Pacejka 96 Model

#### 3.3.3.1 Inputs to the Pacejka 96 Model

The following inputs are required to compute the longitudinal force  $F_x$  using the Magic Formula:

- $x_u$  : Unsprung mass position
- $\sigma_d$  : Slip ratio (input to calculate longitudinal slip).
- $F_{z,\text{tire}}$  : Normal force acting on the tire.
- $\mu$  : Friction coefficient (road-tire interaction).
- $\dot{x}_b$ : Longitudinal velocity of the vehicle body (sprung mass speed).
- $V_{cx}$  : Longitudinal velocity of the sprung mass.
- **n-D**  $T(u)$  : A nonlinear function or look-up table.

#### 3.3.3.2 Outputs from the Pacejka 96 Model

The outputs represent forces computed using the Pacejka Magic Formula:

- $F_x$  : Longitudinal force generated by the tire (traction/braking force).
- $C_{Fk}$  : Additional force coefficient related to Pacejka curve fitting.

Summary of Inputs and Outputs

Inputs	Description
$x_u$	Unsprung mass displacement
$\sigma_d$	Slip ratio (used to calculate slip and traction)
$F_{z,\text{tire}}$	Vertical load on the tire (normal force)
$\mu$	Tire-road friction coefficient
$\dot{x}_b$	Vehicle longitudinal velocity (sprung mass speed)
$V_{cx}$	Longitudinal velocity of the sprung mass
n-D $T(u)$	Nonlinear function

**Table 3.2:** Inputs to the Pacejka 96 Model

Outputs	Description
$F_x$	Tire longitudinal force (traction/braking)
$C_{Fk}$	Additional force coefficient (related to Pacejka parameters)

**Table 3.3:** Outputs from the Pacejka 96 Model

### 3.4 Controllers Design

In this thesis two controllers are used, one is longitudinal controller, one is vertical controller. The longitudinal controller is a pid based controller using slip error as input and output the torque correction to reduce slip, while the vertical controller is a skyhook controller.

#### 3.4.1 longitudinal controller

The longitudinal controller take the current mu value through a look-up table calculate the relatively optimal slip target value then compare with the actual slip value passing through a pid controller to get the torque correction to adjust the motor torque to avoid excessive slip of tire.

The transfer function of the pid controller

$$PID = \frac{200s^2 + 200s + 100}{s^2 + s} \quad (3.16)$$

The **root locus method** is a graphical technique used in control system design to analyze how the locations of a system's closed-loop poles change as a gain or parameter varies; it helps predict system stability and transient response. In tuning the PID controller for the longitudinal slip control, the root locus was used to visualize and adjust the system's dynamic behavior. The PID controller, introduces two zeros and two poles. The zeros shift the root locus branches toward the left-half of the complex plane, enhancing stability and speeding up the response, while the poles filter high-frequency signals to prevent excessive oscillations. By observing the root locus, the PID gains were tuned through trial and error to position the closed-loop poles appropriately—achieving a balance between fast reaction to slip errors and maintaining stability, ensuring effective torque regulation and slip control under varying road conditions.

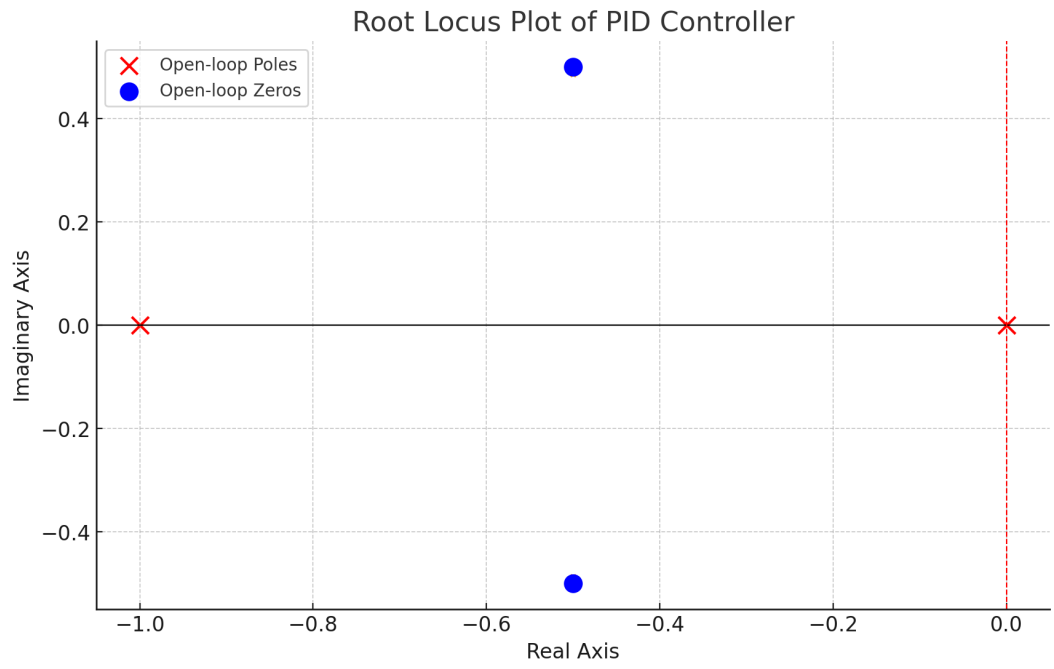


Figure 3.6: Root Locus Plot of PID Controller

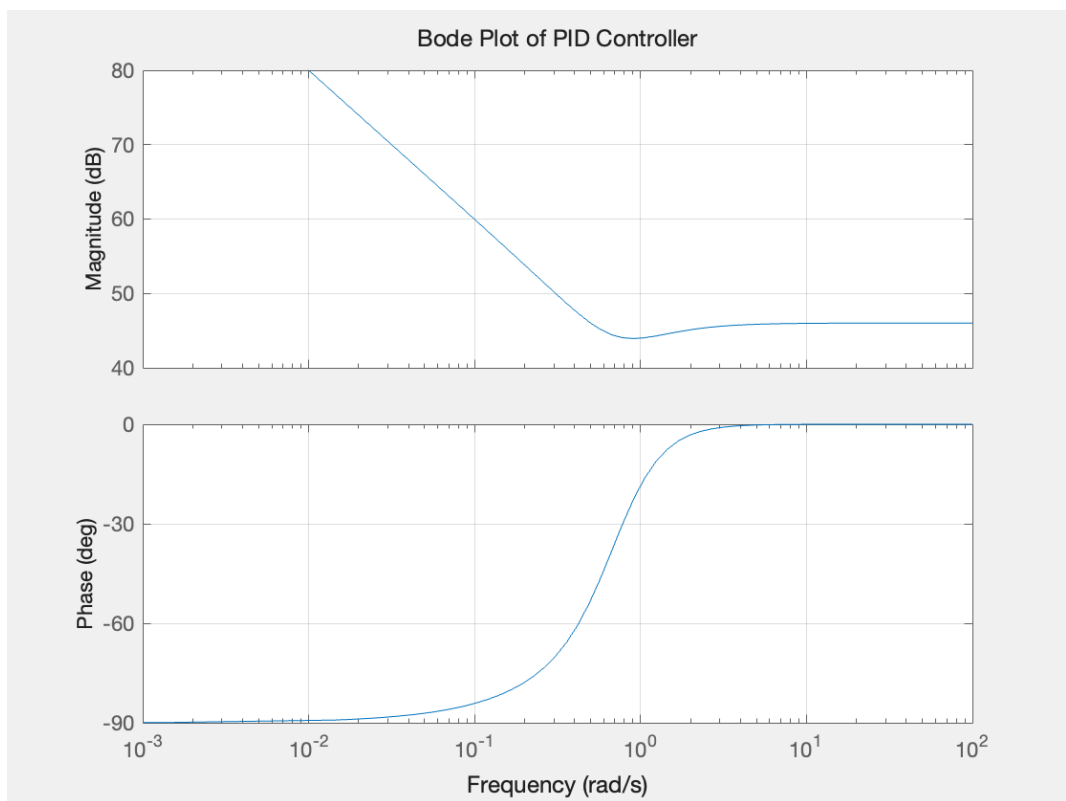


Figure 3.7: bode plot of the pid controller

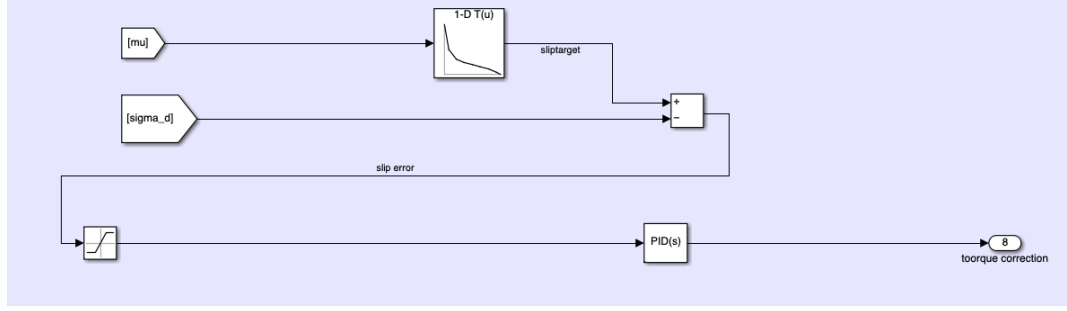


Figure 3.8: Longitudinal controller

### 3.4.2 Vertical controller

The vertical controller that is used is skyhook. Skyhook control is a semi-active suspension strategy that adjusts damping force to stabilize the vehicle body motion while reducing road disturbances, improving both ride comfort and handling performance.

The active control force is given by:

$$F_a = C_s \cdot \dot{z}_b + C_{zf} \cdot (\dot{z}_b - \dot{z}_u) \quad (3.17)$$

where:

- $F_a$  is the active control force.
- $C_s$  is the Skyhook damping coefficient (acting on body velocity  $\dot{z}_b$ ).
- $C_{zf}$  is the relative damping coefficient (acting on  $\dot{z}_b - \dot{z}_u$ , the relative velocity between the body and unsprung mass).
- $\dot{z}_b$  is the body velocity.
- $\dot{z}_u$  is the unsprung mass velocity.

### 3.5 Road Profiles and Simulation Scenarios

#### 3.5.1 ISO 8608 Class C road

ISO 8608 is an international standard that classifies road surface roughness using Power Spectral Density (PSD). This method measures road irregularities at different spatial wavelengths. The standard has eight roughness classes (A to H). Class A means very smooth highways, and Class H means very rough off-road terrains. Most paved secondary roads, like ISO Class C roads, are in Class C or D. These have moderate roughness and are good for standard passenger vehicles. Road roughness is measured with profilometers, accelerometers, or laser scanning systems. This data helps engineers check ride comfort, tire durability, and suspension performance.

In this thesis first two road profile ISO 8608 class c road are used ,one is used to test the effect of the introduce of big unsprung mass ,second is used to test the effectiveness of the controllers ,first profile is 100 m long with constant mu 0.8, second one ranging from 0-100 m, first 50 meter the mu is 0.8, from 50-100 meter the mu is 0.17.



**Figure 3.9:** iso c class road profile

#### 3.5.2 Three bumps

This road profile is a 100m road there are three bumps placed at 20m 40m and 60m, the road friction is varying accross the road, showing as the figure , below the road profile is a zoomed in of bump.

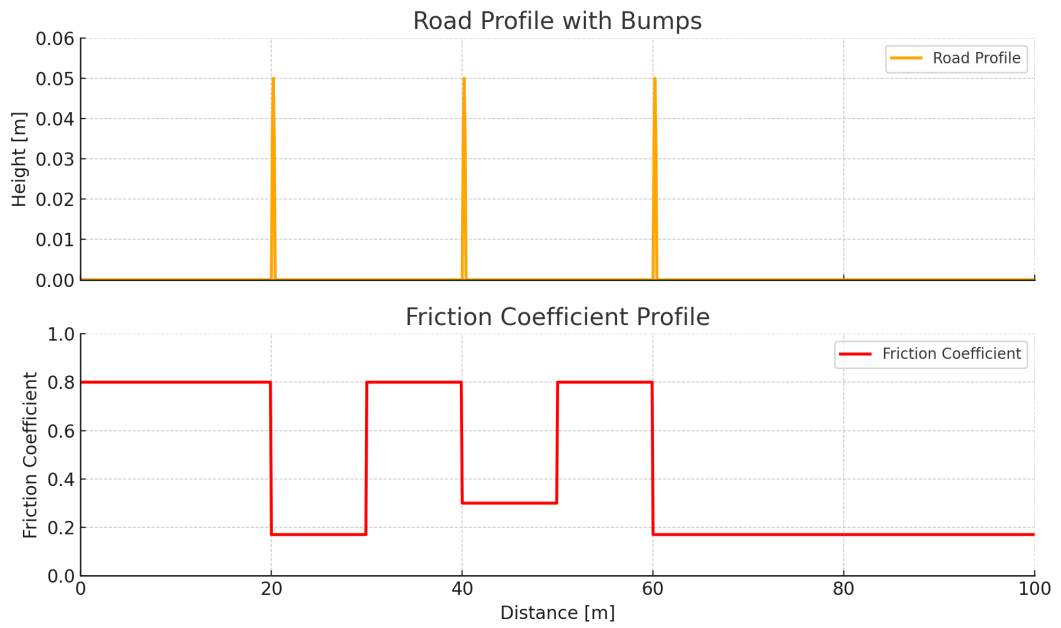


Figure 3.10: three bumps profile

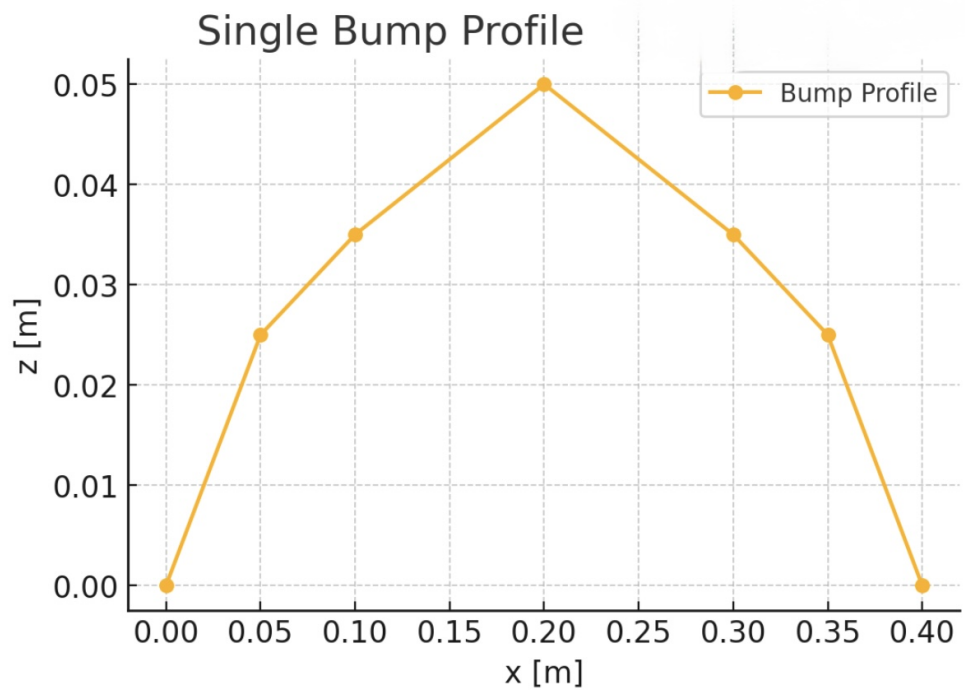


Figure 3.11: zoomed in single bump

### 3.5.3 Simulation Scenarios

In the section above we generate the road profile with  $x$  and  $z$  but in the quarter model implemented the input is  $\omega$  and  $\beta$  so here we need to introduce the enveloping model

### 3.6 Road Profile Enveloping Model

The enveloping model[6] is used to process road irregularities and determine the effective road profile that influences the vehicle dynamics. It provides an improved representation of how the tire interacts with uneven road surfaces.

Effective Road Height

$$w(x_u) = \frac{Z_{e,fc} + Z_{e,rc}}{2} - b_c \quad (3.18)$$

where:

- $Z_{e,fc}$  and  $Z_{e,rc}$  are the **vertical positions** of the front and rear ellipse centers.
- $b_c$  is the **vertical semi-axis** of the ellipses.

Effective Road Gradient

$$\tan(\beta_y(x_u)) = \frac{Z_{e,fc} - Z_{e,rc}}{l_s} \quad (3.19)$$

where:

- $l_s$  is the **longitudinal spacing** between the front and rear ellipses.

Front and Rear Ellipse Equations

$$\left(\frac{x_{e,fc}}{a_c}\right)^c + \left(\frac{z_{e,fc}}{b_c}\right)^c = 1 \quad (3.20)$$

where:

- $a_c, b_c$  are the **horizontal and vertical semi-axes** of the ellipse.
- $c$  is an **ellipse shape parameter**.

Final Computation of the Contact Patch Profile

The maximum height of the road profile at each ellipse is calculated as:

$$Z_{e,fc} = \max(z_r(x_w, x_{e,fc}) + d_{fc}(x_{e,fc})), \quad x_{e,fc} \in [-a_c, a_c] \quad (3.21)$$

$$Z_{e,rc} = \max(z_r(x_w, x_{e,rc}) + d_{rc}(x_{e,rc})), \quad x_{e,rc} \in [-a_c, a_c] \quad (3.22)$$

where:

$$d_{rc}(x_{e,rc}) = b_c \left(1 - \left(\frac{|x_{e,rc}|}{a_c}\right)^c\right)^{\frac{1}{c}} \quad (3.23)$$

$$d_{fc}(x_{e,fc}) = b_c \left(1 - \left(\frac{|x_{e,fc}|}{a_c}\right)^c\right)^{1/c} \quad (3.24)$$

are the distance from the ellipse center to its bottom boundary.

### 3.7 Key Performance Indicators (KPIs)

To test the performance of the vehicle under different conditions, separate kpis are established, first are the vertical acceleration of the sprung mass adjusted to ISO 2631 Weighted Acceleration (m/s<sup>2</sup>) ISO 2631 is an international standard that evaluates human response to whole-body vibration. It applies frequency-dependent weighting functions to raw acceleration signals to reflect how vibrations of different frequencies affect human perception and comfort. The weighted acceleration is calculated using a transfer function.

#### 3.7.1 Sprung-mass weighted vertical acceleration

$$a_w = W(f) \cdot a \quad (3.25)$$

where:

- $a_w$  is the weighted acceleration (m/s<sup>2</sup>),
- $W(f)$  is the frequency weighting function,
- $a$  is the raw acceleration (m/s<sup>2</sup>).

#### 3.7.2 Road holding index

The second kpi is rhi, the Road Holding Index (RHI) quantifies the ability of a vehicle's suspension to maintain contact with the road surface. It is defined as

$$RHI = \frac{k_{tf} \cdot (z_u - w)}{m \cdot g} \quad (3.26)$$

where:

- $RHI$  is the road holding index (dimensionless),
- $k_{tf}$  is the tire stiffness (N/m),
- $z_u$  is the unsprung mass displacement (m),
- $w$  is the road displacement (m),
- $m$  is the total mass (kg),
- $g$  is the gravitational acceleration (m/s<sup>2</sup>).

#### 3.7.3 Maximum slip

The third kpi is the max sigma(slip) The maximum slip is important for assessing traction performance, stability.

definition of slip

$$\lambda = \frac{V_w - V_x}{V_x} \times 100\% \quad (3.27)$$

### 3.7.4 Slip error integral

and the last slip error integral. The slip error integral is used to measure how much the actual slip deviates from the desired slip over time.

$$I_{\text{slip}} = \int_0^T (\lambda_{\text{desired}} - \lambda_{\text{actual}}) dt \quad (3.28)$$

where:

- $I_{\text{slip}}$  is the slip error integral (dimensionless),
- $\lambda_{\text{desired}}$  is the target slip ratio (%),
- $\lambda_{\text{actual}}$  is the actual slip ratio (%),
- $T$  is the time period (s).

A lower slip error integral indicates better slip control and improved vehicle stability.

# Chapter 4

## Results and Discussion

### 4.1 KPI Analysis

#### 4.1.1 ISO class c road with constant friction coefficient ( testing influence of heavier unsprung mass )

This road profile is used to test **how the increased unsprung mass would effect the vehicle dynamics performance** in term of the kpis.

**Table 4.1:** Influence of performance of IWM

Parameter	Big Unsprung Mass (extra IWM 24kg)	Little Unsprung Mass (No IWM)
$a_{w,rms}(m/s^2)$	$3.908 \times 10^{-1}$	$3.839 \times 10^{-1}$
$RHI_{rms}$	$1.010 \times 10^{-3}$	$9.560 \times 10^{-4}$
$\lambda_{max}$	$1.978 \times 10^{-2}$	$1.535 \times 10^{-2}$
$I_{slip}$	$4.540 \times 10^{-2}$	$3.810 \times 10^{-2}$

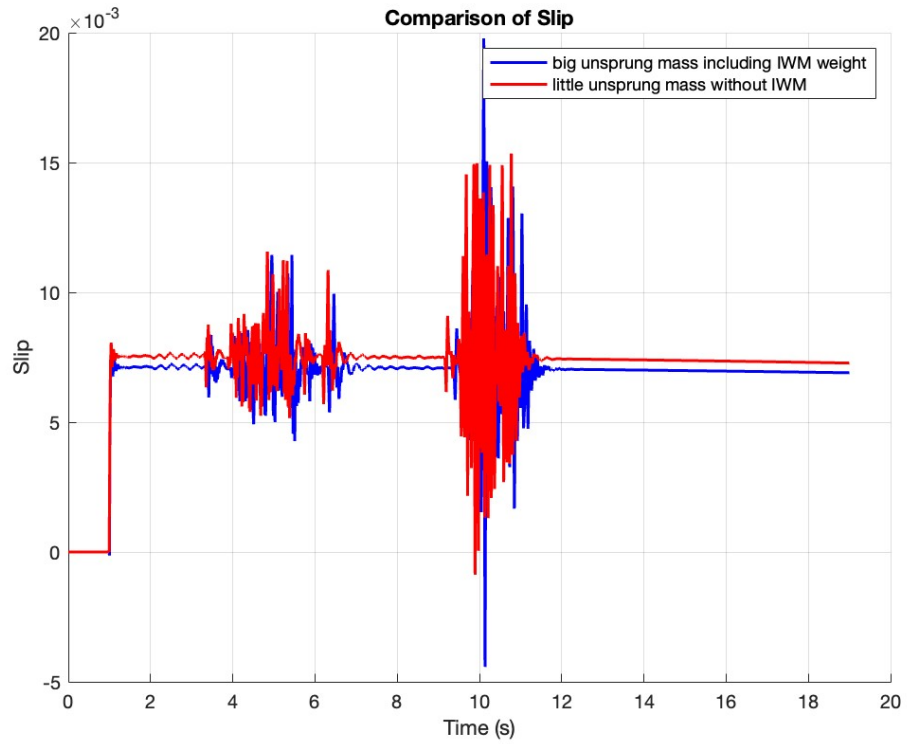


Figure 4.1: comparison of slip with and without IWM

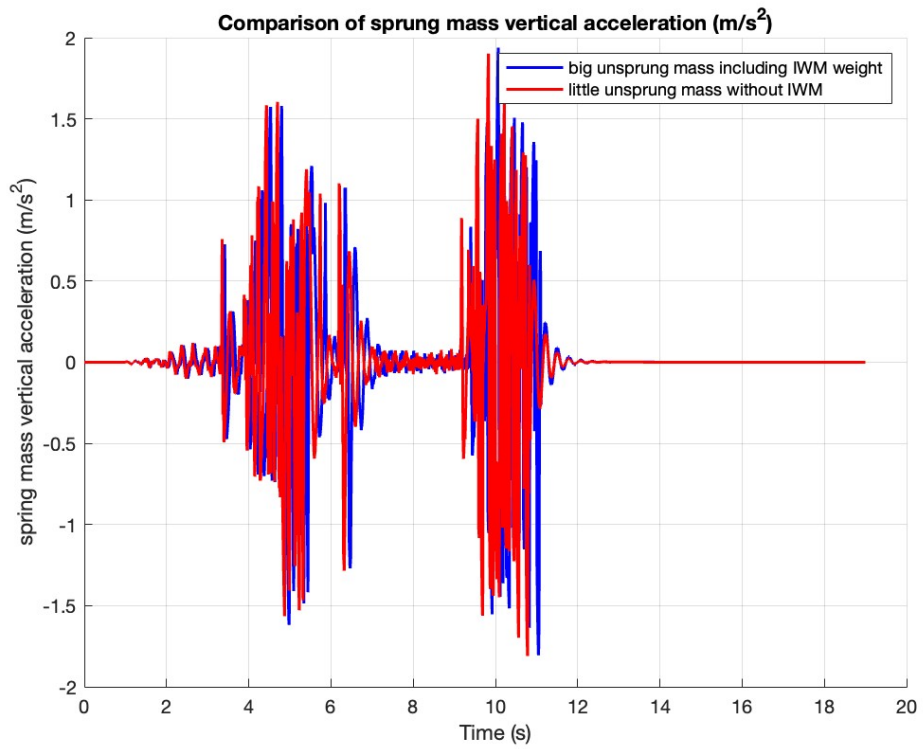
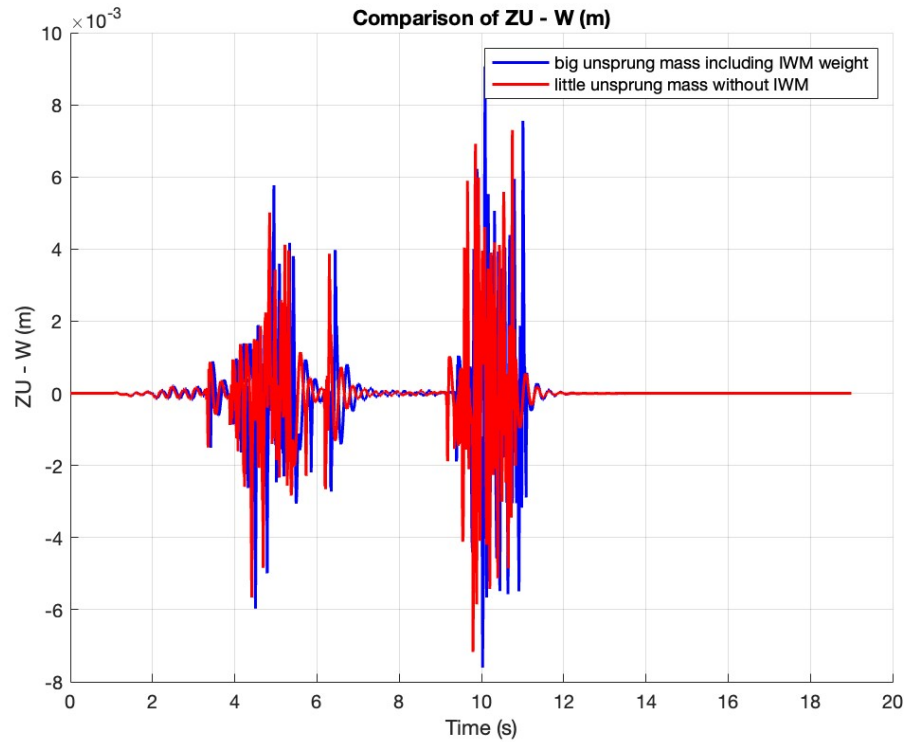


Figure 4.2: comparison of sprung mass vertical acceleration with and without IWM



**Figure 4.3:** comparison of zu-w with and without IWM

From the table and figs we observe that with the extra unsprung mass due to IWM all the performance become worse.

#### 4.1.1.1 Comfort Analysis

The vertical acceleration is slightly higher with a larger unsprung mass (0.39082 vs. 0.38398  $m/s^2$ ), increasing by approximately 1.75%.

This means more road bumps are felt inside the car when the unsprung mass is larger. A heavier unsprung mass makes it harder for the wheel to follow the road surface, forcing the suspension to work harder and resulting in a bumpier ride. In short, a greater unsprung mass reduces ride comfort, making passengers feel more road vibrations. Reducing unsprung mass helps improve ride quality by allowing the wheels to move more smoothly over uneven surfaces.

#### 4.1.1.2 Handling Performance

The road holding index decreases when the unsprung mass is larger (0.001010 vs. 0.000956), dropping by 5.35%.

This is evident in the ZU-W graph, which shows increased wheel movement with a higher unsprung mass. A heavier unsprung mass leads to greater fluctuations in tire force, making it harder for the tire to maintain consistent road contact. This reduces grip and negatively impacts cornering performance. In short, a larger unsprung mass worsens handling, as the tire loses contact with the road more frequently. Reducing

unsprung mass improves stability and enhances cornering performance.

#### **4.1.1.3 Stability and Slip Control**

Slip error increases by 16.08% when the unsprung mass is lower ( $0.0381 \rightarrow 0.0454$ ). However, with a larger unsprung mass, slip variations become much more erratic, as seen in the high-frequency spikes of the blue curve. A heavier unsprung mass makes slip harder to control during braking and acceleration.

With more inertia, the wheel takes longer to adjust to sudden speed changes, leading to greater slip variations. This instability makes it more challenging for traction control systems to maintain grip. Increased slip oscillations also reduce the effectiveness of ABS and traction control.

Reducing unsprung mass helps improve braking and acceleration stability, making vehicle control more precise.

#### **4.1.1.4 Necessity of Implications for TCS and Vertical Control Strategies**

Large unsprung mass affects both horizontal (traction) and vertical (comfort and stability) dynamics. This makes advanced control strategies necessary because the extra weight makes it harder for the wheels to stay in contact with the road. Traction Control Systems (TCS) help by reducing slip changes through quick torque adjustments, but this alone is not enough to fully stabilize the vehicle. Vertical control methods like Skyhook damping or semi-active suspension systems are also needed to reduce extra movements and keep the wheels steady on rough surfaces. Without these systems, the vehicle may experience stronger vibrations and instability, making driving less comfortable and less safe. A combined system that uses both TCS and adaptive suspension provides better control by managing both slip and ride comfort at the same time. This ensures good performance in different driving situations, helping the vehicle stay stable during acceleration, braking, and cornering.

#### **4.1.2 ISO 8608 class c road with decreased friction coefficient ( $\mu$ )**

**This road profile is to test the effectiveness and the influence of the controllers.**

performance analysis of different control strategies under an 100m ISO Class C road with decreased friction coefficient ( $\mu$ ) at 50m. Three configurations were tested:

- Uncontrolled (Passive Damper)

With Two Controllers (Skyhook + TCS)

Only with Longitudinal Controller (TCS) (TCS+passive damper)

**The following Key Performance Indicators (KPIs) were analyzed:**

- $a_{w,rms}$ (m/s<sup>2</sup>): Measures ride comfort. Lower values indicate better comfort.

- $\mathbf{RHI}_{\text{rms}}$ : Measures handling performance. Lower values indicate better tire contact with the road.
- $\lambda_{\text{max}}$ : Measures the peak slip value. Lower values indicate better traction and stability.
- $I_{\text{slip}}$ : Measures accumulated slip error. Lower values are preferable.

The performance of each configuration is summarized in Table 4.3.

<b>KPI</b>	<b>Uncontrolled</b>	<b>Skyhook + TCS</b>	<b>TCS Only</b>
$a_{w,\text{rms}}(\text{m/s}^2)\downarrow$	$5.075 \times 10^{-1}$	<b><math>3.189 \times 10^{-1}</math></b>	$5.070 \times 10^{-1}$
$\mathbf{RHI}_{\text{rms}}\downarrow$	$1.222 \times 10^{-3}$	$1.357 \times 10^{-3}$	<b><math>1.221 \times 10^{-3}</math></b>
$\lambda_{\text{max}}\downarrow$	$8.853 \times 10^{-1}$	$5.448 \times 10^{-2}$	<b><math>4.105 \times 10^{-2}</math></b>
$I_{\text{slip}}\downarrow$	$8.262 \times 10^0$	$3.040 \times 10^{-2}$	<b><math>2.650 \times 10^{-2}</math></b>

**Table 4.2:** Performance Comparison of Different Control Strategies

#### 4.1.2.1 Comfort Analysis

The Skyhook + TCS setup makes the ride much more comfortable, lowering  $a_{w,\text{rms}}(\text{m/s}^2)$  from 0.50747 to 0.31891, which is a 37.2% reduction.

The TCS-only setup does not make the ride smoother. It works almost the same as the passive damper.

#### 4.1.2.2 Handling Performance

Since a lower Road Holding Index (RHI) is better, the TCS only configuration provides the best handling performance.

The Skyhook + TCS configuration slightly worsens handling, likely due to introduced oscillations.

#### 4.1.2.3 Stability and Slip Control

Both Skyhook + TCS and TCS Only greatly reduce slip, but TCS Only performs the best in terms of slip control. The  $I_{\text{slip}}$  clearly shows that TCS Only provides the most effective slip control, with a 99.68% reduction compared to the uncontrolled setup.

This means that using TCS Only significantly reduces the amount of slip, making the vehicle much more stable and improving overall performance on the road.

#### 4.1.2.4 Conclusion

For Comfort: Skyhook + TCS is the best choice. It reduces vertical acceleration  $a_{w,\text{rms}}(\text{m/s}^2)$  by 37.16%, making the ride much smoother and more comfortable for passengers.

For Handling: TCS Only provides the best road contact. The Road Holding Index (Rhi rms) is slightly lower (0.08% improvement), which means the vehicle maintains better grip on the road surface, leading to better handling performance.

For Stability and Traction: TCS Only is the most effective. It reduces  $\lambda_{\max}$  by 95.36%, showing a major improvement in stability and traction, which helps the vehicle maintain control even in challenging driving conditions.

The Passive Damper performs the worst in all aspects. It does not improve comfort, handling, or stability, making it the least effective option among the three setups.

Overall, if comfort is prioritized, Skyhook + TCS is preferable. However, if handling and stability are more critical, TCS Only is the best choice.

In the figs down below the blue represents only passive, red is skyhook+TCS , green is only TCS (TCS+passive damper)

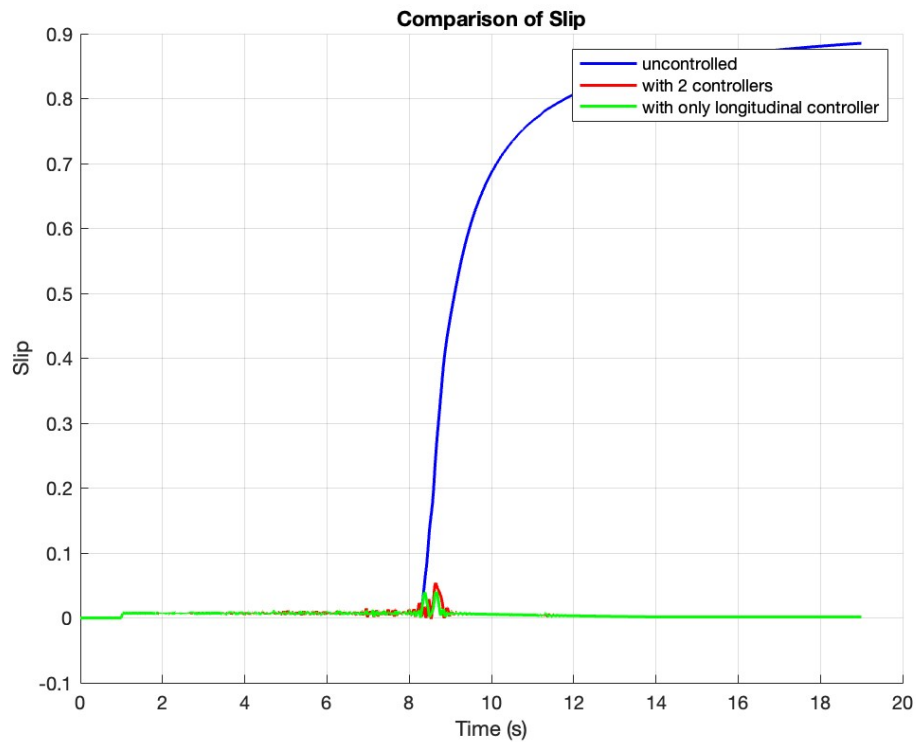


**Figure 4.4:** slip of ISO C road with changing  $\mu$

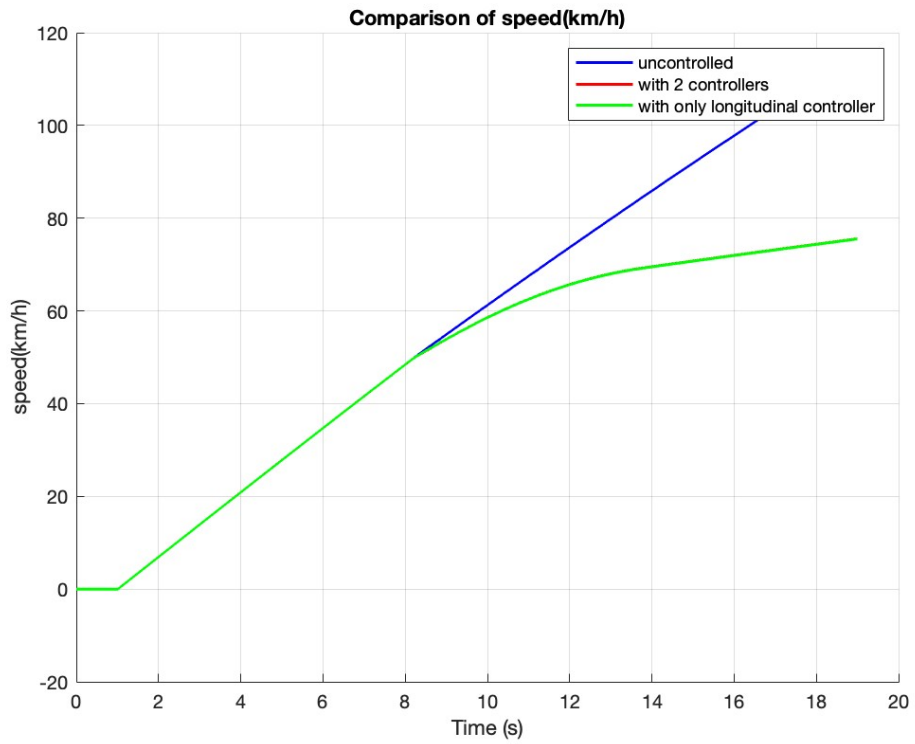


Figure 4.5: longitudinal speed of ISO class c road with changing  $\mu$

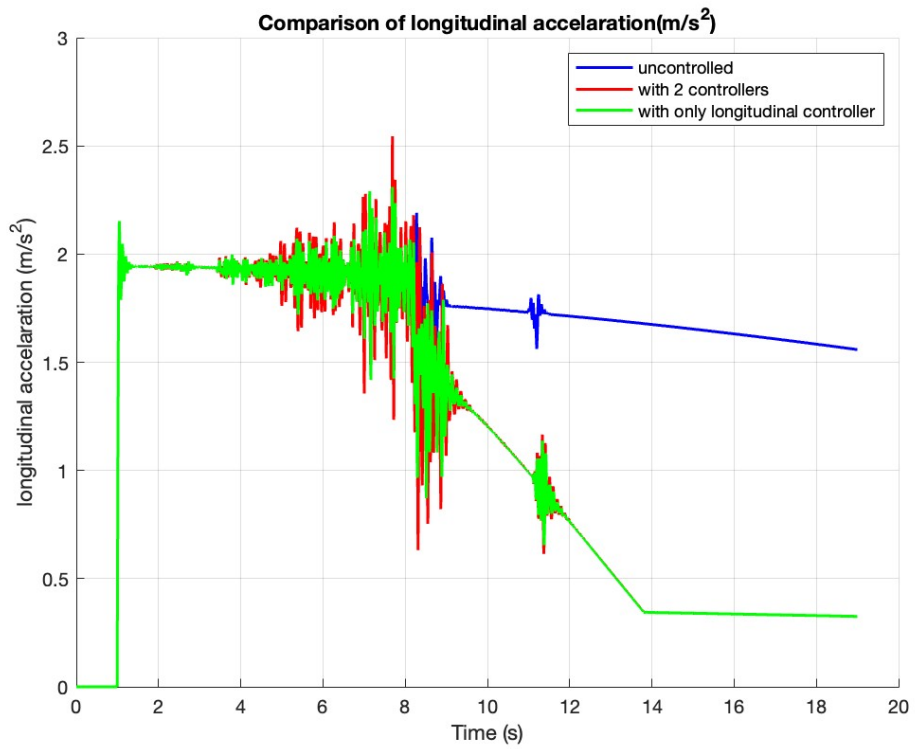


Figure 4.6: longitudinal acceleration of slip of ISO C road with changing  $\mu$

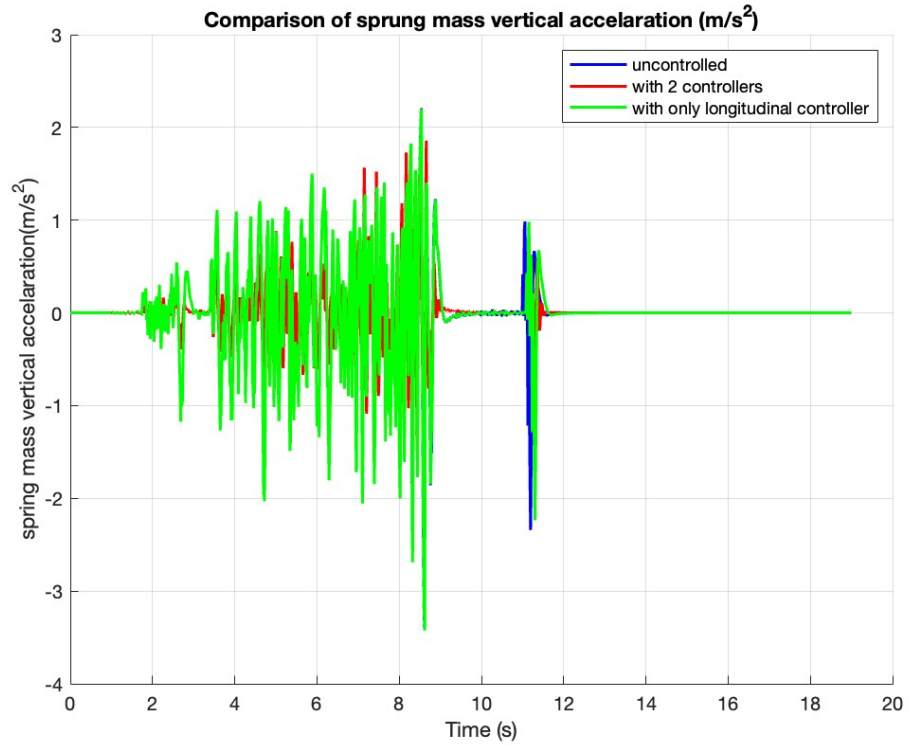


Figure 4.7: sprung mass vertical acceleration of ISO class c road with changing  $\mu$

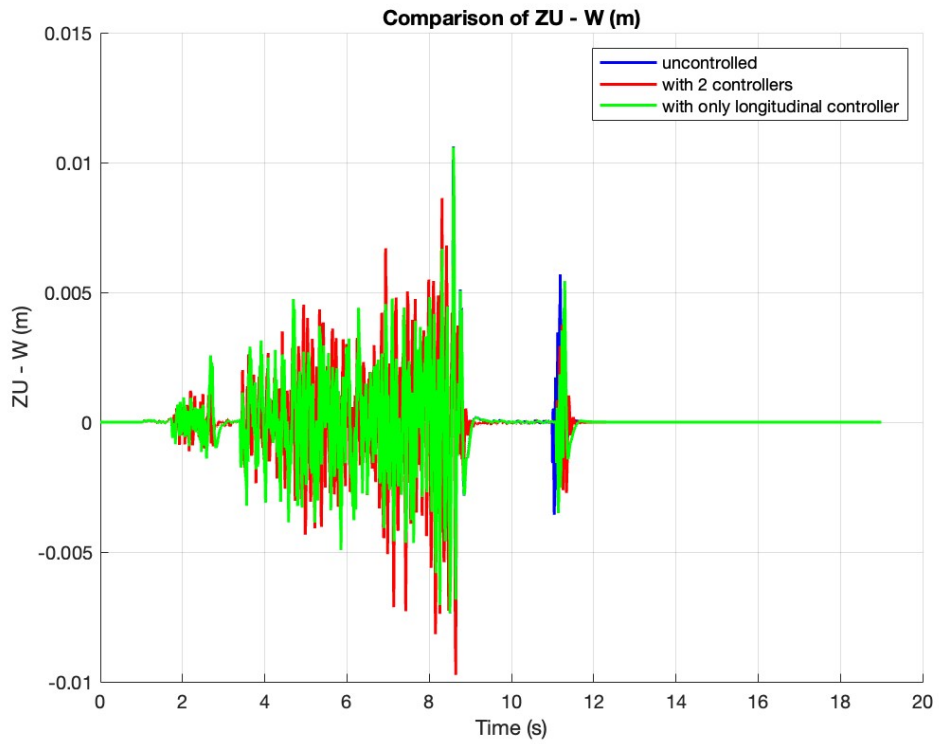
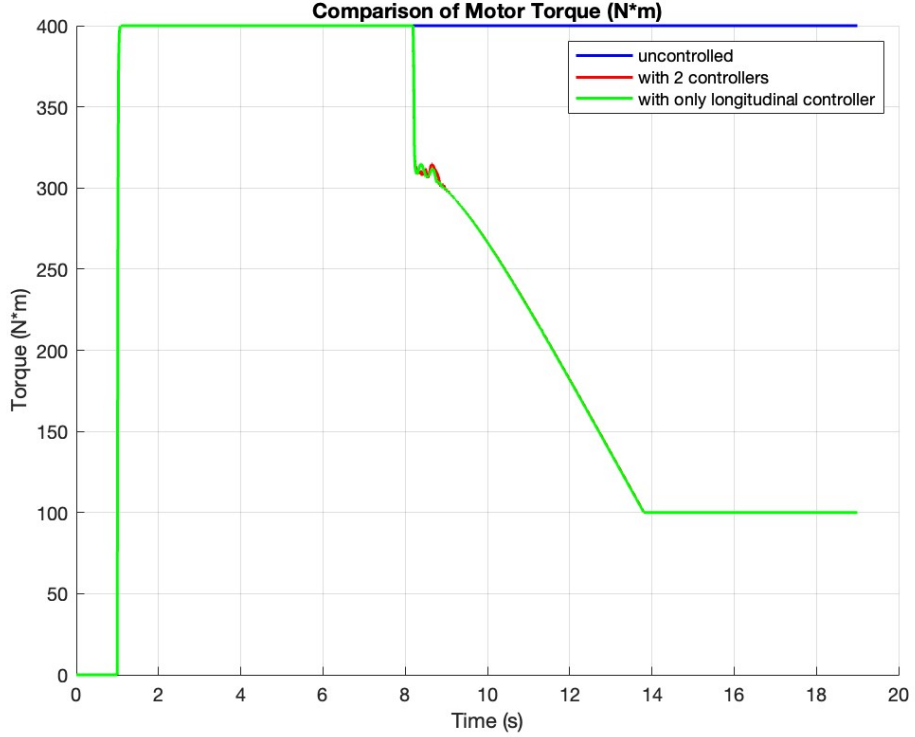


Figure 4.8: zu-w of ISO class c road with changing  $\mu$



**Figure 4.9:** motor torque of ISO class c road with changing  $\mu$

TCS alone proves to be the most effective in maintaining stability, traction, and road holding, as it keeps slip near zero, regulates torque application, and minimizes variations in ZU - W, ensuring consistent tire-ground contact. Skyhook + TCS improves ride comfort by reducing vertical oscillations in the sprung mass acceleration, although it introduces fluctuations in longitudinal acceleration. It is important to note that the Skyhook system is primarily designed to enhance comfort rather than improve road holding or handling.

The uncontrolled system performs the worst, with excessive slip, particularly after 8s, leading to complete traction loss, unstable acceleration, poor road holding, and an inability to effectively regulate torque. In terms of speed, the uncontrolled system reaches the highest velocity but at the cost of stability, whereas TCS moderates acceleration to prevent traction loss, and Skyhook + TCS provides a balanced approach. While TCS alone ensures superior grip control and smooth acceleration, it does not enhance comfort as much as the Skyhook system.

Additionally, the Skyhook controller plays a role in managing suspension responses, indirectly improving stability but not directly affecting road holding. When evaluating torque application, TCS proves crucial in adapting to slip conditions, while the uncontrolled system applies excessive torque before rapidly losing traction.

Overall, the combination of Skyhook and TCS provides the best balance between ride comfort, handling stability, and traction control. However, TCS alone is indispensable for maintaining grip and preventing slip under low-friction conditions.

### 4.1.3 Three bumps with decreased friction coefficient ( $\mu$ )

This road profile is a 100m road there are three bumps placed at 20m 40m and 60m, the road friction is varying across the road as mentioned in

**Three configurations were tested:**

- Uncontrolled (Passive Damper)
- With Two Controllers (Skyhook + TCS)
- Only with Longitudinal Controller (TCS)(TCS+passive damper)

**The following Key Performance Indicators (KPIs) were analyzed:**

- $a_{w,peaktopeak}$  (m/s<sup>2</sup>): Measures ride comfort. Lower values indicate better comfort.
- $RHI_{peaktopeak}$ : Measures handling performance. Lower values indicate better tire contact with the road.
- $\lambda_{max}$ : Measures the peak slip value. Lower values indicate better traction and stability.
- $I_{slip}$  : Measures accumulated slip error. Lower values are preferable.

The performance of each configuration is summarized in Table 4.3.

KPI	Uncontrolled	Skyhook + TCS	TCS Only
$a_{w,peak\ to\ peak}$ (m/s <sup>2</sup> )↓	$1.072 \times 10^1$	<b><math>8.320 \times 10^0</math></b>	$1.073 \times 10^1$
$RHI_{peak\ to\ peak}$ ↓	$9.860 \times 10^{-2}$	$1.079 \times 10^{-1}$	<b><math>9.856 \times 10^{-2}</math></b>
$\lambda_{max}$ ↓	$8.784 \times 10^{-1}$	$6.137 \times 10^{-1}$	<b><math>1.370 \times 10^{-1}</math></b>
$I_{slip}$ ↓	$8.096 \times 10^0$	$4.402 \times 10^{-1}$	<b><math>4.420 \times 10^{-2}</math></b>

**Table 4.3:** Performance Comparison of Different Control Strategies on Road with Three Bumps and Variable Friction

#### 4.1.3.1 Comfort Analysis

The Skyhook + TCS setup makes ride comfort better. This is clear from the lower  $a_{w,peaktopeak}$  (m/s<sup>2</sup>) value (8.3204, 22.35% lower than uncontrolled). It helps reduce the shaking caused by road bumps.

The TCS Only setup does not make vertical comfort better. Its  $a_{w,peaktopeak}$  (m/s<sup>2</sup>) value (10.7335) is almost the same as the uncontrolled case (0.16% higher). It works like a passive damper.

#### 4.1.3.2 Handling Performance

Since a lower Road Holding Index (Rhi) is better, the TCS Only setup gives the best handling. Its  $RHI_{peaktopeak}$  value is 0.098558, which is 0.04% lower than uncontrolled.

The Skyhook + TCS setup makes handling slightly worse. Its  $RHI_{\text{peaktopeak}}$  value (0.10794) is 9.47% higher than uncontrolled. This is likely because of the added damping effects.

#### 4.1.3.3 Stability and Slip Control

Both Skyhook + TCS and TCS Only greatly reduce slip, but TCS Only works best.

The  $I_{\text{slip}}$  shows that TCS Only provides the most effective slip control. Its value (0.0442) is 99.45% lower than uncontrolled. The Skyhook + TCS value (0.4402) is also much lower, 94.56% lower than uncontrolled.

#### 4.1.3.4 Conclusions

For Comfort: Skyhook + TCS is the best choice, reducing impact from bumps.

For Handling: TCS Only provides the best road contact, ensuring stable tire-ground interaction.

For Stability and Traction: TCS Only is the most effective, preventing excessive slip in low-friction regions.

Passive Damper performs the worst in all aspects, failing to manage both ride comfort and traction stability.

In the figures below: Blue shows only the passive damper, Red is Skyhook + TCS. Green is TCS Only (TCS+passive damper).

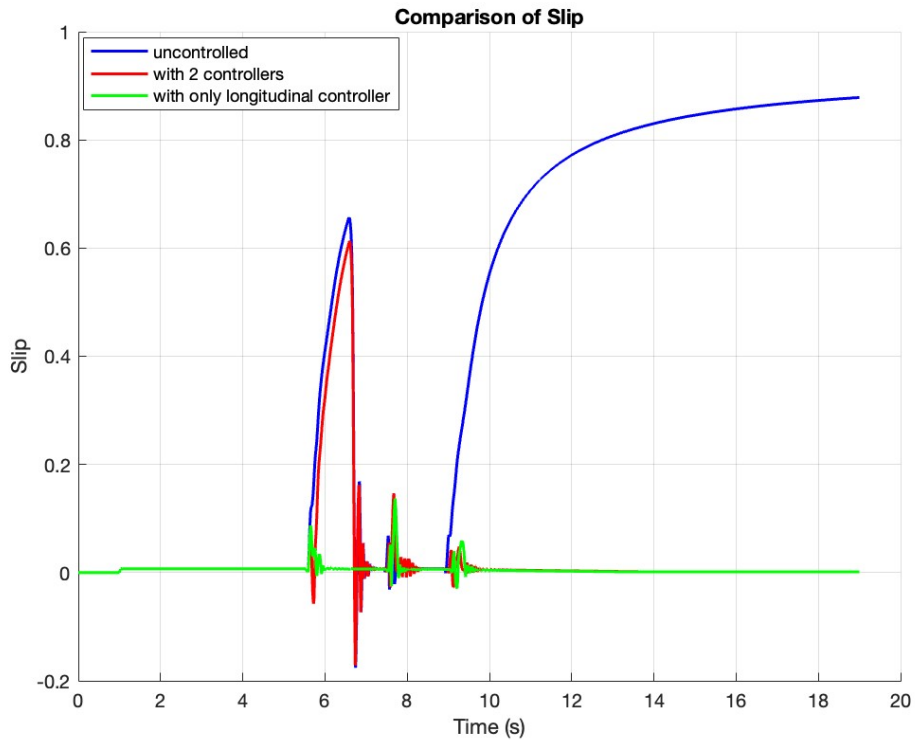


**Figure 4.10:** slip of three bumps with decreased friction coefficient

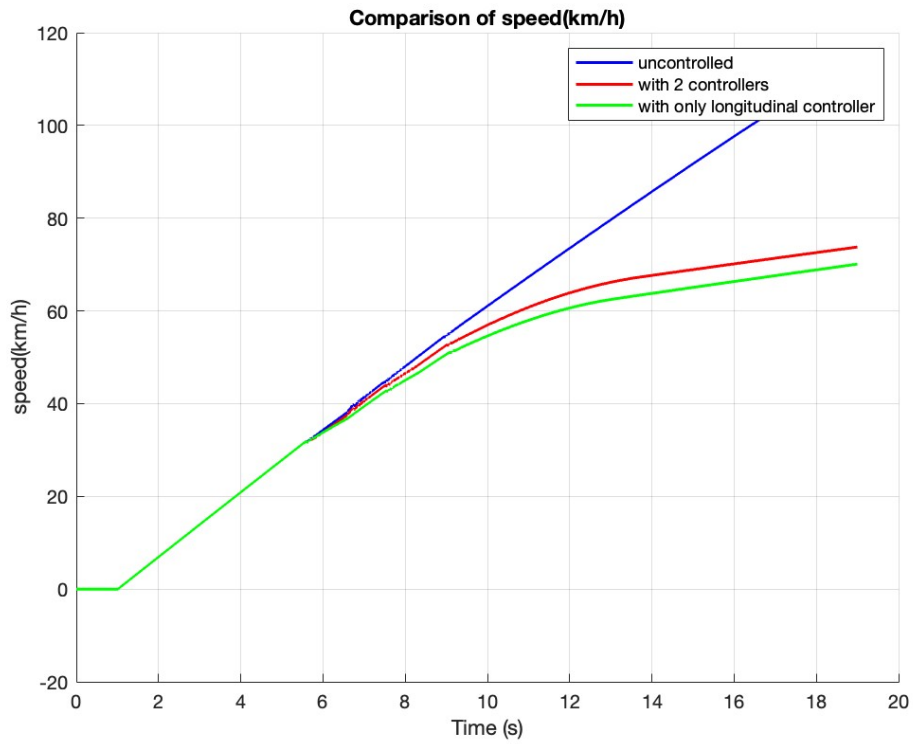


Figure 4.11: longitudinal speed of three bumps with decreased friction coefficient

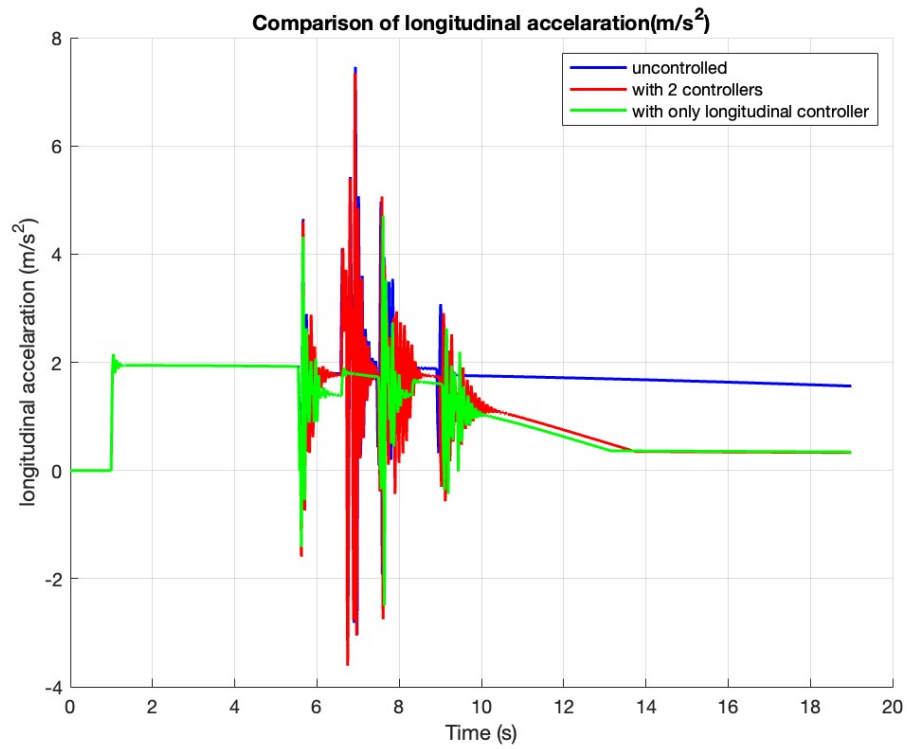
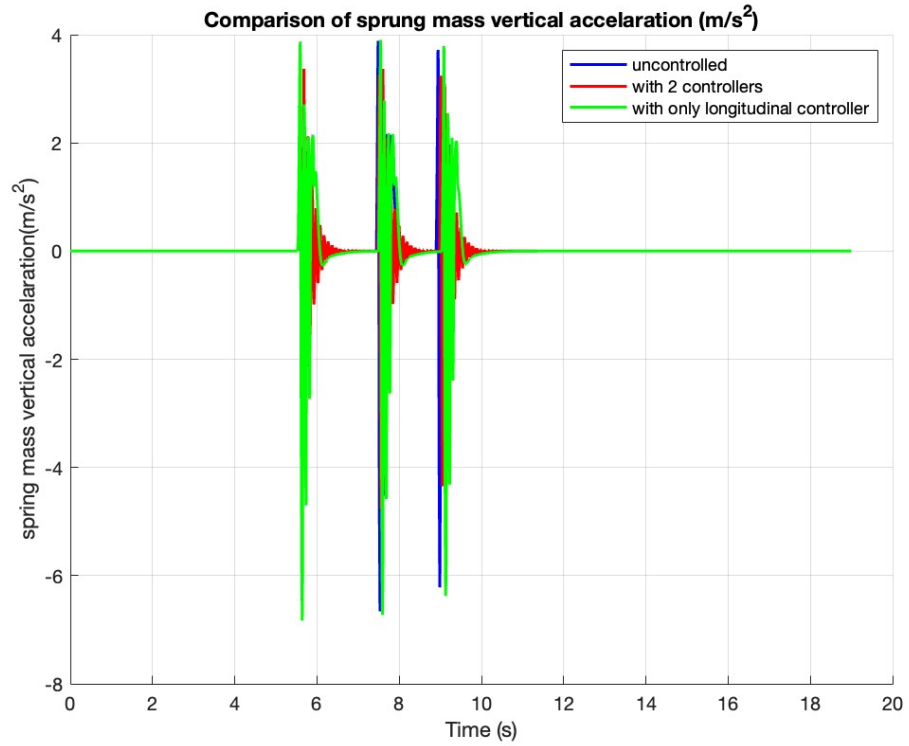
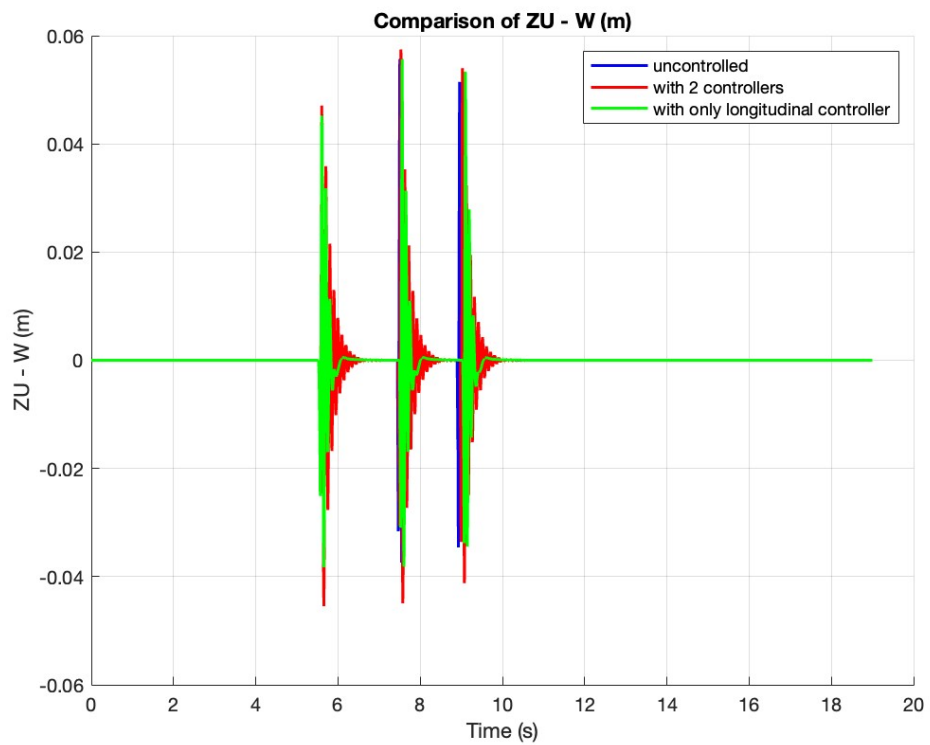


Figure 4.12: longitudinal acceleration of three bumps with decreased friction coefficient



**Figure 4.13:** sprung mass vertical acceleration of three bumps with decreased friction coefficient



**Figure 4.14:** zu-w of three bumps with decreased friction coefficient

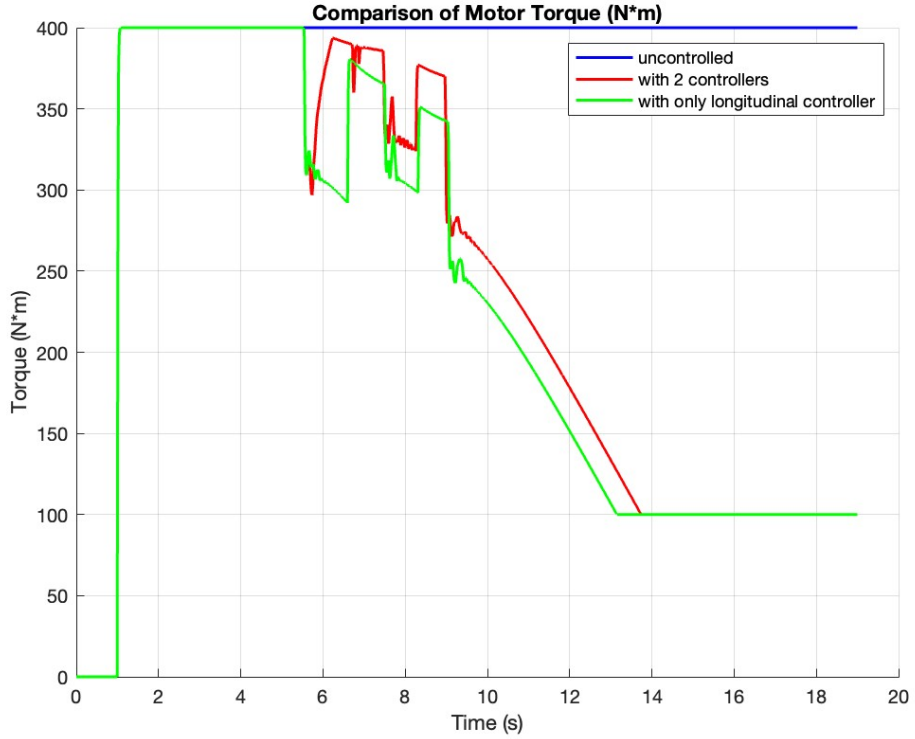


**Figure 4.15:** motor torque of three bumps with decreased friction coefficient

In this test, the best choice depends on what is more important.

If comfort matters most, Skyhook + TCS is better. It lowers vertical movement by 22.35% and reduces slip by 94.56%.

If handling and stability are more important, TCS Only is the best. It has the lowest  $RHI_{\text{peaktopeak}}$  (0.04% lower than uncontrolled) and the best slip control ( $I_{\text{slip}}$  99.45% lower than uncontrolled). It helps keep the wheels in contact with the road, even on bumpy surfaces with different friction levels.

# Chapter 5

## Conclusion and future work

### 5.1 Summary of Findings

This study examined how in-wheel motors (IWMs) affect vehicle dynamics. It focused on both longitudinal and vertical performance. A simulation model was built to analyze different conditions. The key points from the results are:

A big unsprung mass makes ride comfort worse. The vehicle feels more vibrations, and the suspension has to work harder to absorb shocks from the road. Handling performance is also affected. The tire loses contact with the road more often, reducing grip and stability, which is crucial for safe driving, especially in sharp turns or on rough surfaces. Slip control becomes harder with a bigger unsprung mass. The vehicle has stronger slip variations, making braking and acceleration less stable, which can lead to safety risks on wet or icy roads.

Adding control systems improves performance. The Traction Control System (TCS) helps maintain stability by adjusting torque in real time effectively to reduce maximum slip up to 95% compare with uncontrolled case. The Skyhook controller reduces vertical vibrations and makes the ride smoother by actively adjusting damping levels effectively reduce the up to 37%. The best setup depends on the priority. If comfort is most important, Skyhook + TCS is the best combination. If handling and stability are more critical, TCS alone performs better by maintaining better road contact and reducing excessive slip.

### 5.2 Future research directions

#### 5.2.1 Future Research Directions

This research presents a foundational study on longitudinal and vertical dynamics control in in-wheel motor electric vehicles using a simplified quarter-car model. While the results demonstrate the effectiveness of the implemented PID slip controller and Skyhook vertical controller, several opportunities exist to advance the model, enhance control strategies, and explore more comprehensive dynamics. The following directions are recommended for future research:

#### 5.2.1.1 Development of More Complex and High-Fidelity Vehicle Models

The current quarter-car model provides basic insight into the interaction between longitudinal and vertical dynamics. However, to better replicate the complexity of real vehicles and capture more dynamic interactions, future work should focus on developing:

- **Half-Car and Full-Vehicle Models:** By incorporating additional degrees of freedom, such as pitch and roll motions, these models will enable more accurate analysis of dynamic behaviors like weight transfer during acceleration, braking, and cornering. Full-vehicle models also capture lateral dynamics, which are essential for studying combined maneuvers.
- **Multi-Body Dynamics (MBD) Models:** High-fidelity models built using multi-body dynamics software (e.g., ADAMS, Simpack) can simulate complex suspension kinematics, flexible body dynamics, and detailed tire-road interactions. These tools provide realistic environments for control strategy validation and tuning.

#### 5.2.1.2 Advanced Control Strategies

The control methods used in this study (PID and Skyhook) are simple and effective for initial analysis. However, more sophisticated control algorithms can deliver better performance in complex, real-world conditions:

- **Nonlinear Model Predictive Control (NMPC):** NMPC optimizes control inputs by solving an online constrained optimization problem based on predictions from a nonlinear vehicle model. It enables coordinated control of longitudinal slip and vertical suspension forces, considering actuator limitations and changing road conditions.
- **Sliding Mode Control (SMC) and Adaptive Control:** SMC offers strong robustness against model uncertainties and external disturbances, making it suitable for variable road surfaces. Adaptive controllers can adjust control parameters in real-time based on variations in vehicle mass, tire characteristics, and road friction.
- **Learning-Based Controllers:** Deep Reinforcement Learning (DRL) and other data-driven approaches can be trained to manage both longitudinal and vertical dynamics in uncertain environments. These controllers can learn optimal control policies from simulation and adapt them to real-time driving conditions.

#### 5.2.1.3 Integrated Longitudinal and Vertical Dynamics Control

This study treated longitudinal and vertical dynamics as separate control problems. However, these dynamics are inherently coupled in practice. Future work should explore integrated control strategies, including:

- **Coordinated Control Frameworks:** A unified control architecture that simultaneously optimizes longitudinal traction (slip ratio) and vertical ride comfort (body acceleration) can maximize overall vehicle performance. This can be implemented using multi-objective optimization techniques.
- **Predictive and Preview Control:** By leveraging road profile information from onboard sensors (LiDAR, cameras) or vehicle-to-infrastructure (V2X) communication, controllers can predict upcoming road conditions and proactively adjust both motor torque and suspension damping forces.
- **Multi-Objective Optimization:** Trade-offs between competing objectives, such as ride comfort, traction, and handling, can be systematically addressed using multi-objective NMPC or optimization-based control frameworks.

#### 5.2.1.4 Experimental Validation and Real-Time Implementation

Simulation studies must eventually be validated in real-time environments. Future work should focus on:

- **Hardware-in-the-Loop (HIL) Testing:** HIL platforms enable real-time testing of controllers on physical hardware using simulated vehicle models. This step is crucial for verifying computational efficiency and robustness prior to deployment in real vehicles.
- **On-Road Testing:** Final validation of control strategies should be conducted through vehicle testing under various road conditions to assess real-world performance in terms of safety, ride comfort, and stability.

#### 5.2.1.5 Summary

Future research directions aim to enhance the fidelity of vehicle models, leverage advanced control techniques, integrate longitudinal and vertical control, and validate methods in real-time environments. These steps are necessary to address the challenges posed by increased unsprung mass in in-wheel motor electric vehicles and to realize the full potential of distributed drive systems.

# Bibliography

- [1] T. Z. Shi, D. F. Wang, and S. M. Chen. “Investigation of negative influences on ride comfort performance of in-wheel motor vehicles with high unsprung mass”. In: *Proceedings of the 2015 International Conference on Power Electronics and Energy Engineering (PEEE 2015)*. Atlantis Press, 2015, pp. 115–117. DOI: 10.2991/peee-15.2015.31 (cit. on pp. 3–5).
- [2] Peibao Wu, Rongkang Luo, Zhihao Yu, and Zhichao Hou. “Research on the unsprung mass effect of in-wheel motor drives based on a half-vehicle model”. In: *Journal of Tsinghua University (Science and Technology)* 64.8 (2024), pp. 1445–1455. DOI: 10.16511/j.cnki.qhdxxb.2024.21.016 (cit. on pp. 3–5).
- [3] Martyn Anderson and Damian Harty. “Unsprung Mass with In-Wheel Motors – Myths and Realities”. In: *Proceedings of the 10th International Symposium on Advanced Vehicle Control (AVEC 2010)*. Loughborough, UK, 2010, pp. 261–266 (cit. on pp. 5, 6, 9).
- [4] Saber Salem and Amir Yassin. “Sensorless based SVPWM-DTC of AFPMSM for electric vehicles”. In: *Scientific Reports* 12 (May 2022), p. 9023. DOI: 10.1038/s41598-022-12825-x (cit. on p. 7).
- [5] Liqiang Jin, Yajuan Yu, and Yiliang Fu. “Study on the ride comfort of vehicles driven by in-wheel motors”. In: *Advances in Mechanical Engineering* 8.3 (2016), pp. 1–9 (cit. on pp. 7–9).
- [6] Victor Vidal, Pietro Stano, Gaetano Tavolo, Miguel Dhaens, Davide Tavernini, Patrick Gruber, and Aldo Sornioti. “On Pre-Emptive In-Wheel Motor Control for Reducing the Longitudinal Acceleration Oscillations Caused by Road Irregularities”. In: *IEEE Transactions on Vehicular Technology* 71.9 (2022), pp. 9322–9335. DOI: 10.1109/TVT.2022.3172172 (cit. on pp. 8, 9, 18, 28).
- [7] Yechen Qin, Chuan He, Xinxing Shao, Haiping Du, Chuan Xiang, and Ming Dong. “Vibration mitigation for in-wheel switched reluctance motor driven electric vehicle with dynamic vibration absorbing structures”. In: *Journal of Sound and Vibration* 419 (2018), pp. 249–267 (cit. on p. 9).
- [8] Le Van Quynh, Bui Van Cuong, Nguyen Van Liem, Le Xuan Long, and Pham Thi Thanh Dung. “Effect of in-wheel motor suspension system on electric vehicle ride comfort”. In: *Vibroengineering Procedia* 29 (2019), pp. 21–26 (cit. on p. 9).

- [9] Kritika Deepak, Mohamed Amine Frikha, Yassine Benômar, Mohamed El Baghdadi, and Omar Hegazy. “In-Wheel Motor Drive Systems for Electric Vehicles: State of the Art, Challenges, and Future Trends”. In: *Energies* 16.7 (2023), p. 3121. DOI: 10.3390/en16073121 (cit. on p. 9).
- [10] T.K. Bera, K. Bhattacharya, and A.K. Samantaray. “Evaluation of antilock braking system with an integrated model of full vehicle system dynamics”. In: *Simulation Modelling Practice and Theory* 19.10 (2011), pp. 2131–2150. ISSN: 1569-190X. DOI: <https://doi.org/10.1016/j.simpat.2011.07.002>. URL: <https://www.sciencedirect.com/science/article/pii/S1569190X11001237> (cit. on p. 10).
- [11] Rajesh Rajamani. *Vehicle Dynamics and Control*. 2nd. New York, NY: Springer, 2012 (cit. on p. 10).
- [12] Idar Petersen, Tor Arne Johansen, Jörg Kalkkuhl, and Jens Lüdemann. “Wheel slip control in ABS brakes using gain-scheduled constrained LQR”. In: *Proc. of the European Control Conference (ECC)*. Porto, Portugal, 2001 (cit. on p. 11).
- [13] Kanwar Bharat Singh, Mehmet A. Arat, and Saied Taheri. “An Intelligent Tire Based Tire-Road Friction Estimation Technique and Adaptive Wheel Slip Controller for Antilock Brake System”. In: *Journal of Dynamic Systems, Measurement, and Control* 135.3 (2013), p. 031002. DOI: 10.1115/1.4007704 (cit. on p. 11).
- [14] J. P. Den Hartog. *Mechanical Vibrations*. New York: McGraw-Hill, 1956 (cit. on pp. 12, 13).
- [15] R. S. Sharp and D. A. Crolla. “Road Vehicle Suspension Design – A Review”. In: *Vehicle System Dynamics* 16.3 (1987), pp. 167–192 (cit. on pp. 13, 14).
- [16] D. Karnopp, M. J. Crosby, and R. A. Harwood. “Vibration Control Using Semi-Active Force Generators”. In: *ASME Journal of Engineering for Industry* 96.2 (1974), pp. 619–626 (cit. on pp. 13, 14).